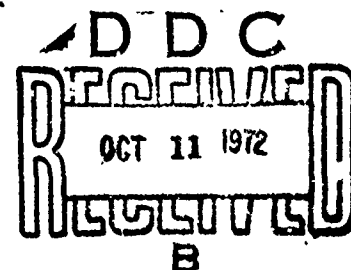AD 749690

A TECHNIQUE FOR THE CALCULATION OF THE OPENING-SHOCK FORCES FOR SEVERAL TYPES OF SOLID CLOTH PARACHUTES

By
William P. Ludtke

20 JUNE 19/2

DDC

RECEIVED

OCT 11 1972

B

NOL

NAVAL ORDNANCE LABORATORY, WHITE OAK, SILVER SPRING, MARYLAND

NOLTR 72-146

DOCUMENT CONTROL DATA - R & D

(Security classification of title, body of abstract and indexing annotation must be entered when the overall report is classified)

1. ORIGINATING ACTIVITY (Corporate author)	2a. REPORT SECURITY CLASSIFICATION
Naval Ordnance Laboratory	UNCLASSIFIED
Silver Spring, Maryland 20910	2b. GROUP

3. REPORT TITLE

A TECHNIQUE FOR THE CALCULATION OF THE OPENING-SHOCK FORCES FOR SEVERAL TYPES OF SOLID CLOTH PARACHUTES

4. DESCRIPTIVE NOTES (Type of report and inclusive dates)

5. AUTHOR(S) (First name, middle initial, last name)

William P. Ludtke

6. REPORT DATE	7a. TOTAL NO. OF PAGES	7b. NO. OF REFS
20 June 1972	71	7

8a. CONTRACT OR GRANT NO.	9a. ORIGINATOR'S REPORT NUMBER(S)
b. PROJECT NO.	NOLTR 72-146
c.	9b. OTHER REPORT NO(S) (Any other numbers that may be assigned this report)
d.	

10. DISTRIBUTION STATEMENT

Approved for public release; distribution is unlimited.

11. SUPPLEMENTARY NOTES	12. SPONSORING MILITARY ACTIVITY

13. ABSTRACT

In 1965, the Naval Ordnance Laboratory was engaged in a project which required the deployment of a 35-foot-diameter extended-skirt parachute (type T-10) as the second stage of a retardation system at an altitude of 100,000 feet. At that time, there were no available data on the T-10 parachute deployed under similar circumstances. This new parachute opening-shock calculation technique was generated as a solution to this dilemma.

A drag area ratio-time ratio signature derived from infinite mass wind-tunnel parachute deployments is combined with Newton's second law of motion to develop instantaneous velocity ratios and shock factors during the deployment process. Methods of computing the reference time (t_o) and the inflation time (t_f) are presented. New concepts of the parachute canopy volume, canopy cloth permeability, parachute initial size at line stretch, and material elasticity are included.

Since the inception of this program, some of the assumptions used in its development have been demonstrated by other experimenters. Other assumptions have not yet been verified. However, the performance predicted by this technique has been in agreement with field test results.

14 KEY WORDS	LINK A		LINK B		LINK C	
	ROLE	WT	ROLE	WT	ROLE	WT
Solid cloth parachutes						
Opening-shock force						
Altitude effects						
Scale factor						
Cloth permeability						
Material elasticity						

NOLTR 72-146

A TECHNIQUE FOR THE CALCULATION OF THE OPENING-SHOCK FORCES FOR
SEVERAL TYPES OF SOLID CLOTH PARACHUTES

Prepared by:
William P. Ludtke

ABSTRACT: In 1965, the Naval Ordnance Laboratory was engaged in a
project which required the deployment of a 35-foot-diameter extended-
skirt parachute (type T-10) as the second stage of a retardation
system at an altitude of 100,000 feet. At that time, there were
no available data on the T-10 parachute deployed under similar
circumstances. This new parachute opening-shock calculation tech-
nique was generated as a solution to this dilemma.

A drag area ratio-time ratio signature derived from infinite mass
wind-tunnel parachute deployments is combined with Newton's second
law of motion to develop instantaneous velocity ratios and shock
factors during the deployment process. Methods of computing the
reference time (t_o) and the inflation time (t_f) are presented. New
concepts of the parachute canopy volume, canopy cloth permeability,
parachute initial size at line stretch, and material elasticity
are included.

Since the inception of this program, some of the assumptions used
in its development have been demonstrated by other experimenters.
Other assumptions have not yet been verified. However, the perform-
ance predicted by this technique has been in agreement with field
test results.

NAVAL ORDNANCE LABORATORY
SILVER SPRING, MARYLAND

NOLTR 72-146   20 June 1972

A TECHNIQUE FOR THE CALCULATION OF THE OPENING-SHOCK FORCES FOR
SEVERAL TYPES OF SOLID CLOTH PARACHUTES

The investigation of this report is related to the calculation of
the opening-shock forces of solid cloth parachutes.

                              ROBERT WILLIAMSON II
                              Captain, USN
                              Commander

                              a. E. Seigel

                              A. E. SEIGEL
                              By direction

CONTENTS

ILLUSTRATIONS

ILLUSTRATIONS (continued)

ILLUSTRATIONS (continued)

TABLES

LIST OF SYMBOLS

A_c — Steady-state projected area of the inflated parachute, ft^2

A_M — Instantaneous canopy mouth area, ft^2

A_{Mc} — Steady-state inflated mouth area, ft^2

a — Acceleration, ft/sec^2

$2\bar{a}$ — Maximum inflated parachute diameter of gore mainseam, ft

b — Minor axis of the ellipse bounded by the major axis ($2\bar{a}$) and the vent of the canopy, ft

b' — Minor axis of the ellipse which includes the skirt hem of the canopy, ft

C — Effective porosity

C_D — Parachute coefficient of drag

C_p — Parachute pressure coefficient, relates internal and external pressure (ΔP) on canopy surface to the dynamic pressure of the free stream

F — Instantaneous force, lbs

F_s — Steady-state drag force that would be produced by a fully open parachute at velocity V_s, lbs

F_c — Constructed strength of the parachute, lbs

F_{max} — Maximum opening-shock force, lbs

g — Gravitational acceleration, ft/sec^2

k — Permeability constant of canopy cloth

m — Mass, slugs

LIST OF SYMBOLS (continued)

M	Mass ratio - ratio of the mass of the retarded hardware (including parachute) to a mass of atmosphere contained in a right circular cylinder of length ($V_s t_o$), face area ($C_D S_o$), and density (ρ)
M'	Mass flow ratio - ratio of atmosphere flowing through a unit cloth area to the atmosphere flowing through a unit inlet area at arbitrary pressure
n	Permeability constant of canopy cloth
P	Cloth permeability - rate of airflow through a cloth at an arbitrary differential pressure, ft^3/ft^2 sec
q	Dynamic pressure, lb/ft^2
S	Instantaneous inflated canopy surface area, ft^2
S_o	Canopy surface area, ft^2
t	Instantaneous time, sec
t_o	Reference time when the parachute has reached the design drag area for the first time, sec
t_f	Canopy inflation time when the inflated canopy has reached its maximum physical size, sec
u	Air velocity through cloth in effective porosity, ft/sec
v	Fictitious theoretical velocity used in effective porosity, ft/sec
V	Instantaneous system velocity, ft/sec
V_o	System velocity at the time $t = t_o$, ft/sec
V_s	System velocity at the end of suspension line stretch, ft/sec
$\underline{V}_o$	Volume of air which must be collected during the inflation process, ft^3
W	Hardware weight, lb
x_i	Instantaneous shock factor

LIST OF SYMBOLS (continued)

X_o Shock factor at the time $t = t_o$

ρ Air density, slugs/ft^3

η Ratio of parachute projected mouth area at line stretch to the steady-state projected area

ϵ Instantaneous elongation

ϵ_{max} Maximum elongation

ϵ_o Initial elongation at the beginning of the elastic phase of inflation

S.F.   Parachute safety factor $= F_c/F_{max}$

INTRODUCTION

In 1965, the Naval Ordnance Laboratory was engaged in a project which utilized a 35-foot-diameter, 10-percent extended-skirt parachute (type T-10) as the second stage of a retardation system for a 250-pound payload. Deployment of the T-10 parachute was to be accomplished at an altitude of 100,000 feet. In this rarefied atmosphere, the problem was to determine the second stage deployment velocity for successful operation. A search of available field test information indicated a lack of data on the solid cloth parachutes at altitudes above 30,000 feet. Also, applying the then existing methods of calculation, the inflation time and opening-shock force to the 100,000-foot altitude situation were questionable.

Utilizing existing wind-tunnel data, low-altitude field test data, and reasonable assumptions, a unique engineering approach to the inflation time and opening-shock problem was evolved that provided satisfactory results. Basically, the method combines a drag area ratio signature as a function of deployment time with Newton's second law of motion to analyze the velocity and force profiles during deployment. The parachute deployment sequence is divided into two phases. The first phase is considered to be inelastic as the parachute inflates initially to its steady-state size for the first time. At this point, it is considered that the elasticity of the parachute materials enters the problem and resists the applied forces until the canopy has reached full inflation.

In this system of analysis, the time (t_o) at which the parachute first achieves its steady-state size is used as the calculation reference time, rather than the more conventional inflation time (t_f). The reference time (t_o) is the time required to collect the inflated steady-state volume of air associated with a canopy of elliptical profile with consideration for the mass flow balance into the inflating canopy mouth and the mass outflow through the inflated portion of the cloth surface area.

The equations developed in this analysis are in agreement with the observed performance of solid cloth parachutes in the field, such as: the decrease of inflation time as altitude increases, effects of altitude on opening-shock force, finite and infinite mass, inflation distance, etc.

DEVELOPMENT OF VELOCITY RATIO AND FORCE RATIO EQUATIONS DURING
THE UNFOLDING PHASE OF PARACHUTE DEPLOYMENT

The necessity for a quick answer to the high altitude inflation time and opening-shock problem dictated a simple engineering approach. It was considered that the parachute deployment would take place in a horizontal attitude in accordance with Newton's second law of motion.

$$\Sigma F = ma$$

$$-\frac{1}{2}\rho V^2 C_D S = \frac{W}{g}\frac{dV}{dt}$$

$$\int_0^t C_D S\, dt = \frac{-2W}{\rho g}\int_{Vs}^V \frac{dV}{V^2} \tag{1}$$

Multiplying the right-hand side of equation (1) by

$$1 = \frac{V_s t_o C_D S_o}{V_s t_o C_D S_o}$$

and rearranging

$$\frac{1}{t_o}\int_0^t \frac{C_D S}{C_D S_o}\, dt = \frac{-2W}{\rho g V_s t_o C_D S_o}\; V_s\int_{V_s}^V \frac{dV}{V^2} \tag{2}$$

In order to integrate the left-hand term of equation (2), the drag area ratio must be defined for the type of parachute under analysis as a function of deployment reference time (t_o).
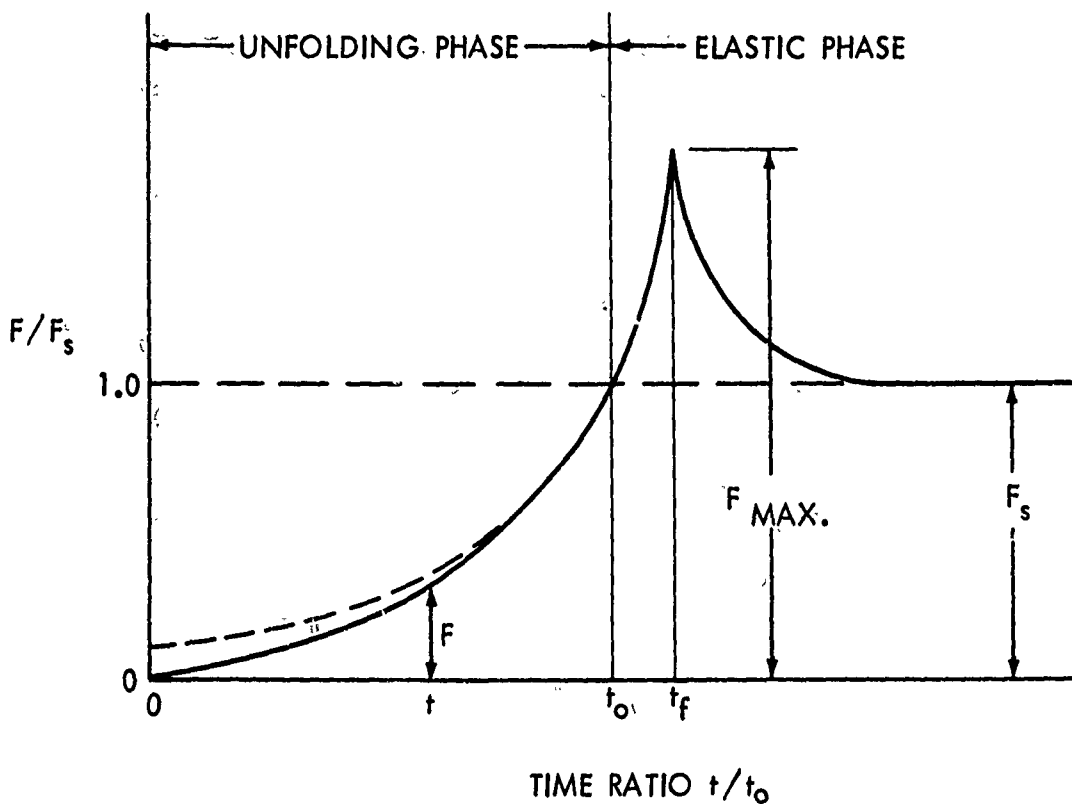
FIG. 1 TYPICAL INFINITE MASS FORCE-TIME HISTORY OF A SOLID CLOTH
PARACHUTE IN A WIND TUNNEL

Figure 1 illustrates a typical force-time history of a solid cloth
parachute deployed in a wind tunnel under infinite mass conditions.
The depicted segment of the opening-shock signature is that portion
which occurs after the snatch force. A parachute is defined to be
fully inflated when the maximum physical size has been attained.
The time at which this occurs is the inflation time (t_f). In the
infinite mass wind-tunnel case, the maximum physical size and shock
force occur at the same time, since the air density and the velocity
are constant during deployment. In the finite mass case, the maximum
physical size and the maximum opening shock do not necessarily occur
at the same time. Since the maximum physical parachute size is
dependent upon the applied load, structural strength, and elasticity
of the parachute materials, a reference opening time (t_o) which can
be considered to be independent of the applied loads is desirable.
The inflation process was divided into two separate phases. The
first phase is called the unfolding phase where the canopy is under-
going changes of shape during inflation. This phase progresses to
reference time (t_o). At reference time (t_o), the canopy is
considered to have attained its fully inflated steady-state shape
for the first time. Additional inflation of the parachute in the
elastic phase is considered to be caused by elongation of the canopy

materials under the applied loads. For purposes of curve fitting, the reference time (t_0) was established on the infinite mass wind-tunnel force-time signature as the first point where the instantaneous force was equal to the steady-state drag (F_s).

At any instant during the unfolding phase, the ratio of instantaneous force (F) to the steady-state drag (F_s) can be determined as a function of the time ratio (t/t_0).

$$F = \frac{1}{2} \rho V^2 C_D S$$

$$F_s = \frac{1}{2} \rho V_s{}^2 C_D S_o$$

Since the velocity and density are constant during infinite mass deployment

$$V = V_s$$

and

$$\frac{F}{F_s} = \frac{C_D S}{C_D S_o}$$

Infinite mass opening-shock signatures of several types of parachutes are presented in Figures 2 through 6. Analysis of these signatures using the force ratio (F/F_s) - time ratio (t/t_0) technique indicated a similarity in the performance of the various solid cloth types of parachutes which were examined. The geometrically porous ring slot parachute displayed a completely different signature as was expected. These data are illustrated in Figure 7. If an initial boundary condition of $C_D S/C_D S_o = 0$ at time $t/t_0 = 0$ is assumed, then, the data can be approximated by fitting a curve of the form

$$\frac{C_D S}{C_D S_o} = \left(\frac{t}{t_o}\right)^6 \tag{3}$$

From a practical point of view, all parachutes have some drag area when line stretch is reached. The value of the drag area at $t/t_0 = 0$ is a variable, depending on the type of deployment that is used and the reproducibility of a given deployment system. Taking this additional variable into account, a more generalized drag area ratio expression was determined

4
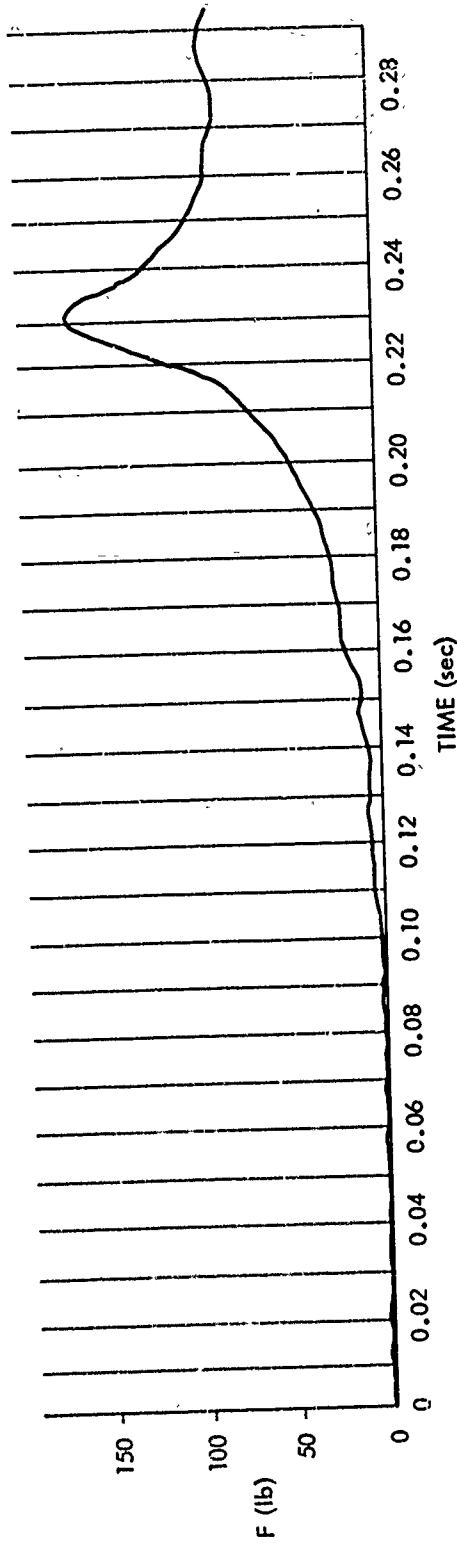
FIG. 2 TYPICAL FORCE-TIME CURVE FOR A SOLID FLAT PARACHUTE
UNDER INFINITE MASS CONDITIONS
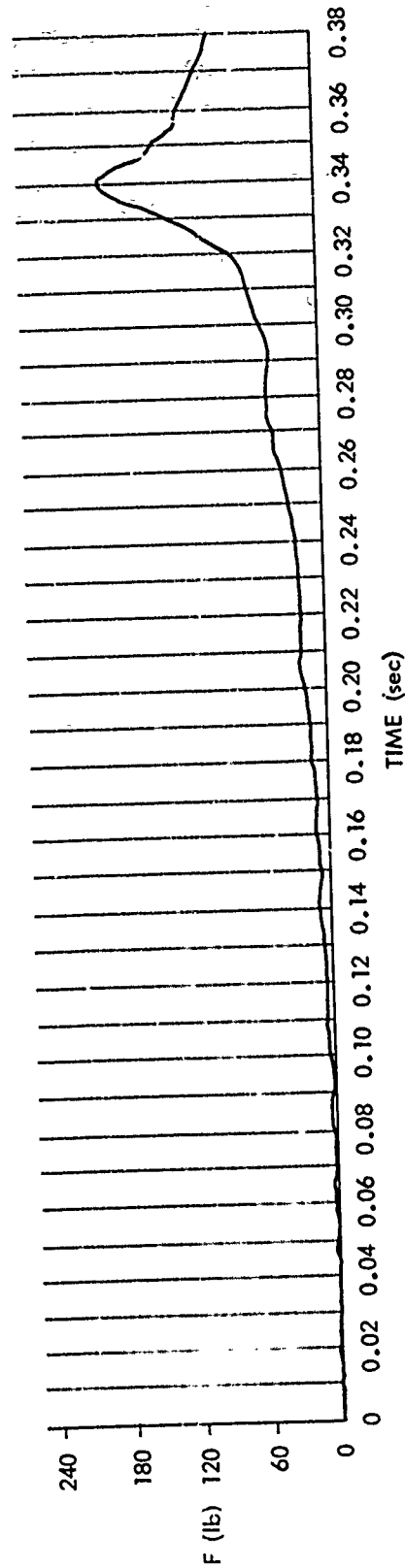
FIG. 3 TYPICAL FORCE-TIME CURVE FOR A 10% EXTENDED SKIRT PARACHUTE
UNDER INFINITE MASS CONDITIONS

REPRODUCED FROM REFERENCE (1)
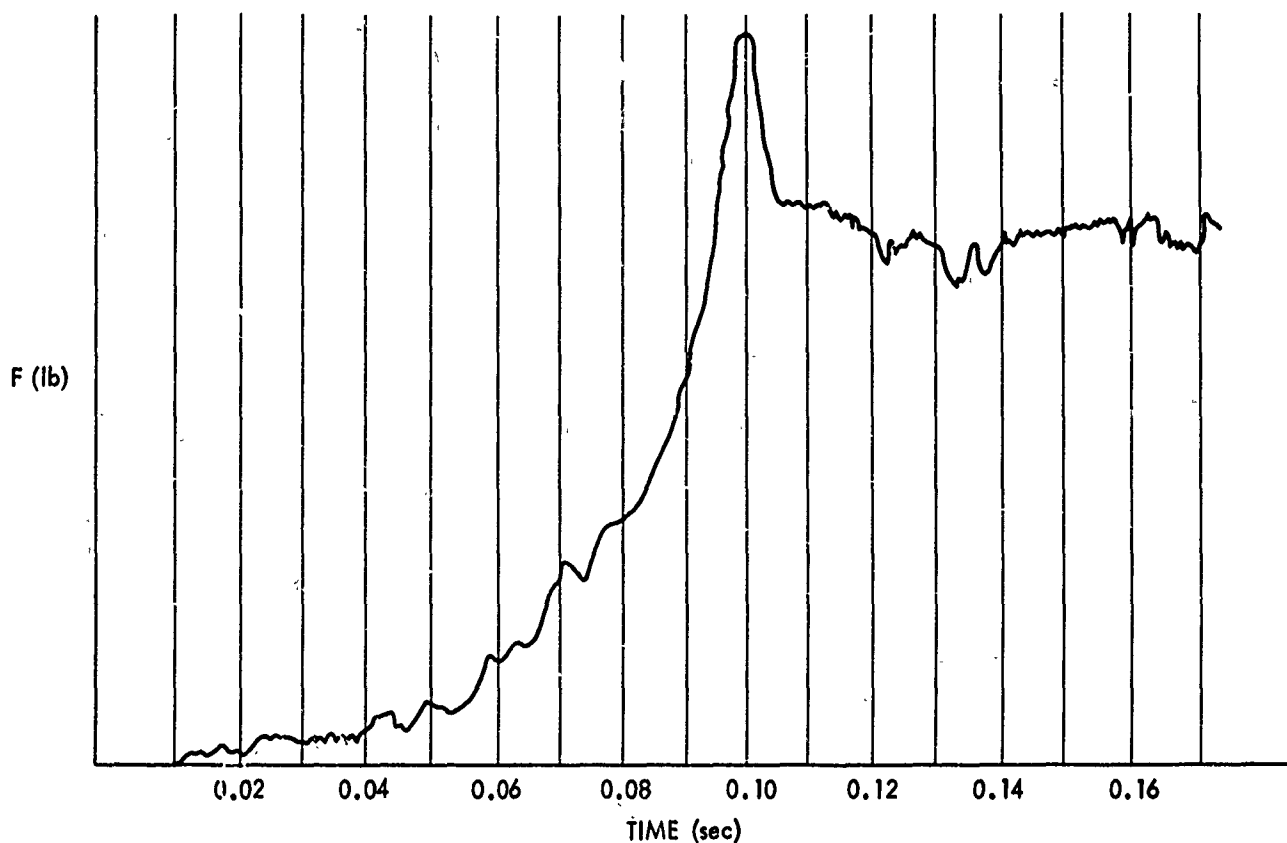
FIG. 4 TYPICAL FORCE-TIME SIGNATURE FOR THE ELLIPTICAL PARACHUTE
UNDER INFINITE MASS CONDITIONS
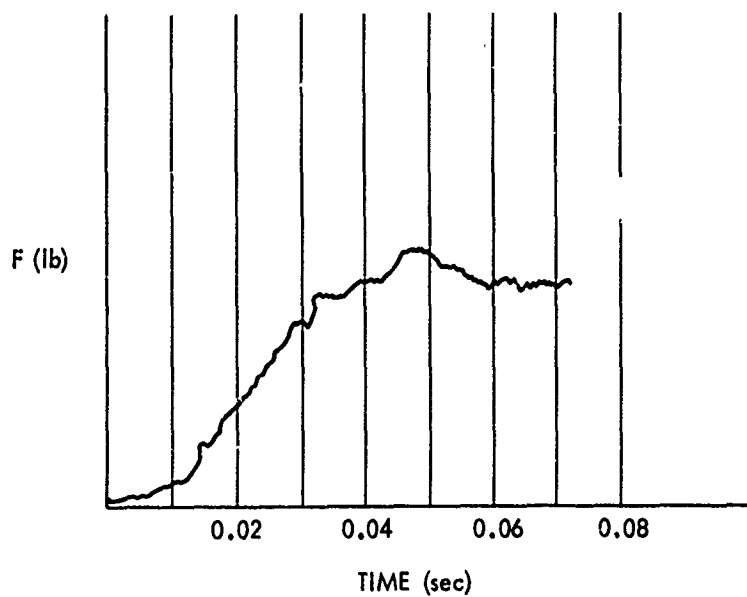
FIG. 5 TYPICAL FORCE-TIME SIGNATURE FOR THE RING SLOT PARACHUTE
20 % GEOMETRIC POROSITY UNDER INFINITE MASS CONDITIONS
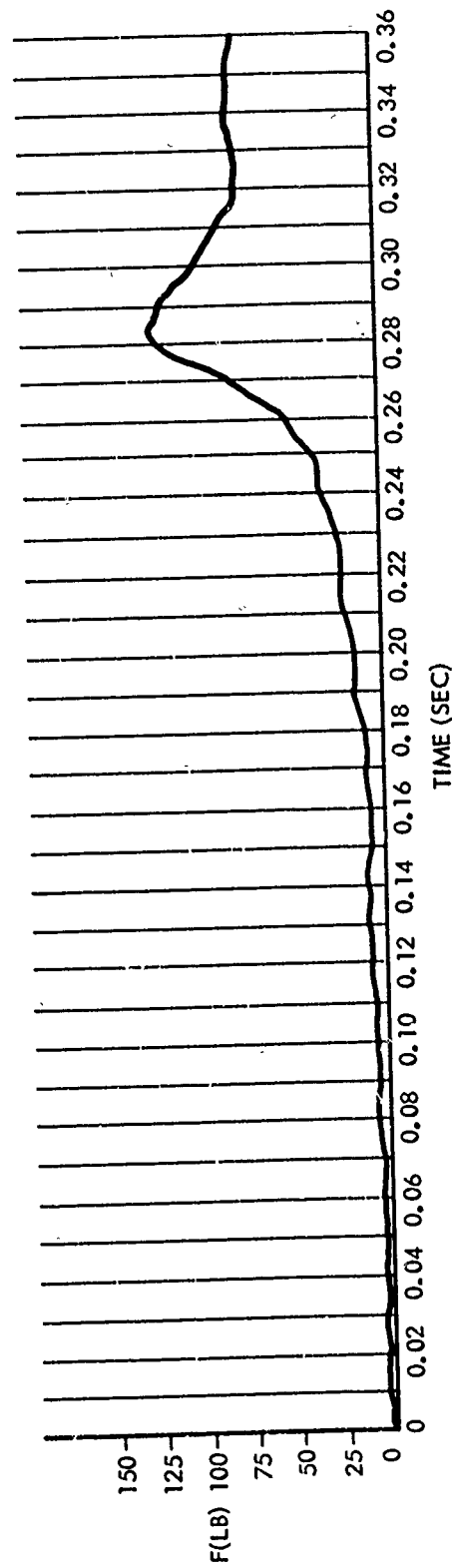
FIG. 6 TYPICAL FORCE-TIME CURVE FOR A PERSONNEL GUIDE
SURFACE PARACHUTE UNDER INFINITE MASS CONDITIONS
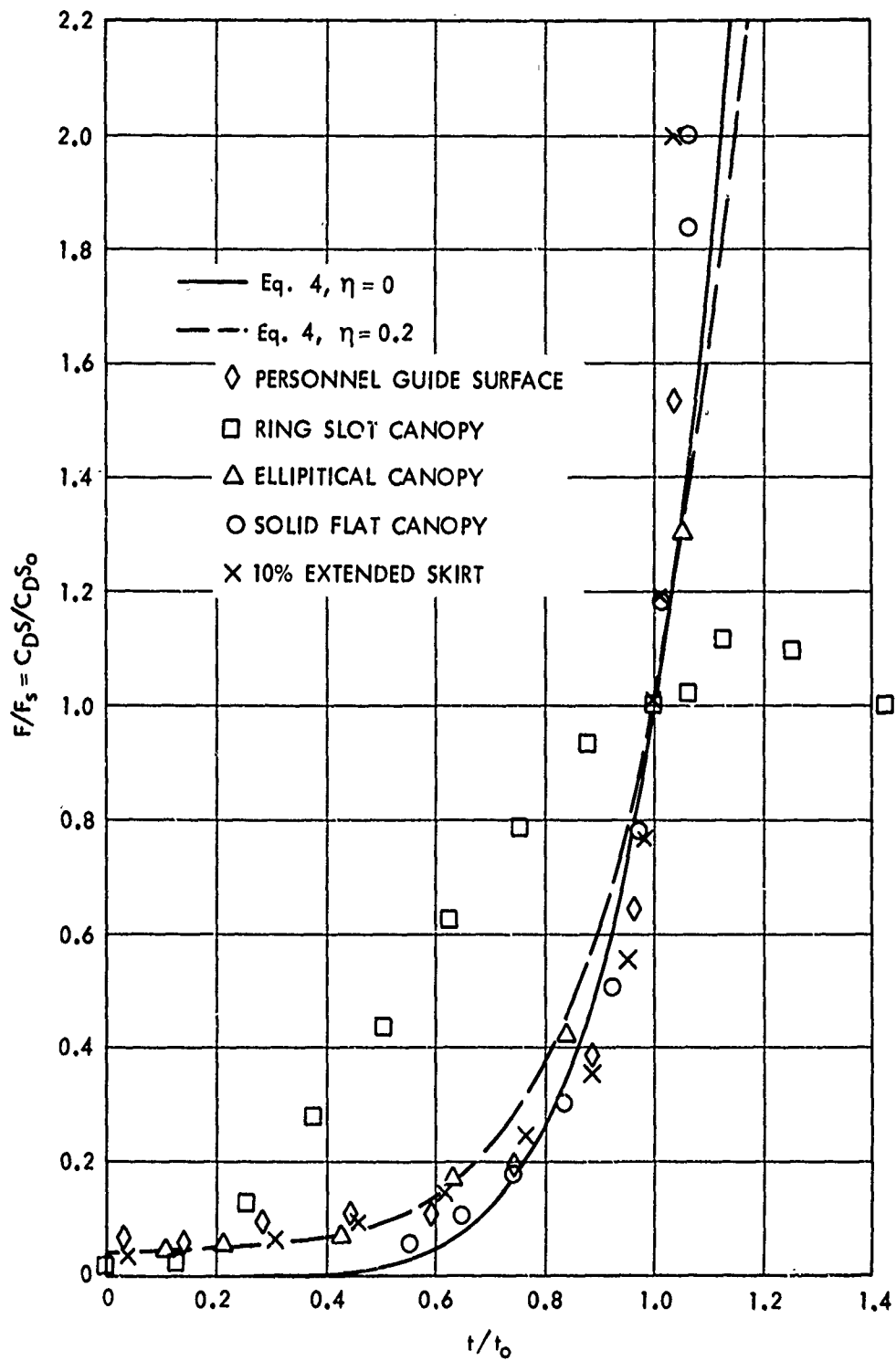
FIG. 7   DRAG AREA RATIO vs TIME RATIO

$$\frac{C_D S}{C_D S_o} = \left[\left(1 - \eta\right)\left(\frac{t}{t_o}\right)^3 + \eta \right]^2 \tag{4}$$

where η is the ratio of the projected mouth area at line stretch to the steady-state projected frontal area. Expanding equation (4)

$$\frac{C_D S}{C_D S_o} = \left(1 - \eta\right)^2 \left(\frac{t}{t_o}\right)^6 + 2\eta \left(1 - \eta\right)\left(\frac{t}{t_o}\right)^3 + \eta^2 \tag{5}$$

At the time that equation (5) was ascertained, it suggested that the geometry of the deploying parachute was independent of density and velocity. It was also postulated that although this expression had been determined for the infinite mass condition that it would also be true for the finite mass case. This phenomenon has since been independently observed and confirmed by Berndt and De Weese in reference (2).

Parachute deployments presented in the force ratio (F/F_S) - time ratio (t/t_o) frame of reference show a repeatability of drag area development not evident in conventional representation. Figure 8 is reproduced from reference (3) and is a composite force-time diagram for a number of tests of the same solid flat parachute under constant test conditions. The three runs indicated are replotted in Figure 9 as ratios of F/F_S versus t/t_o. When viewed in this manner, the percentage of drag area developed for a given percentage of unfolding time is repeatable and conforms with equation (5).

Equation (2) did not include apparent mass or the included mass of the inflating canopy. It was assumed that the effects of these quantities on the deployment characteristics of the parachute are included in the drag area ratio formulation, since it was derived from actual deployment signatures.

The right-hand term of equation (2) contains the expression

$$\frac{2W}{\rho g V_s t_o C_D S_o} = M \tag{6}$$

This term can be visualized as shown in Figure 10 to be a ratio of the retarded mass (including the parachute) to an associated mass of atmosphere contained in a right circular cylinder which is generated by moving an inflated parachute of area $C_D S_o$ for a distance equal to the product of $V_s t_o$ in an atmosphere of density (ρ).

9
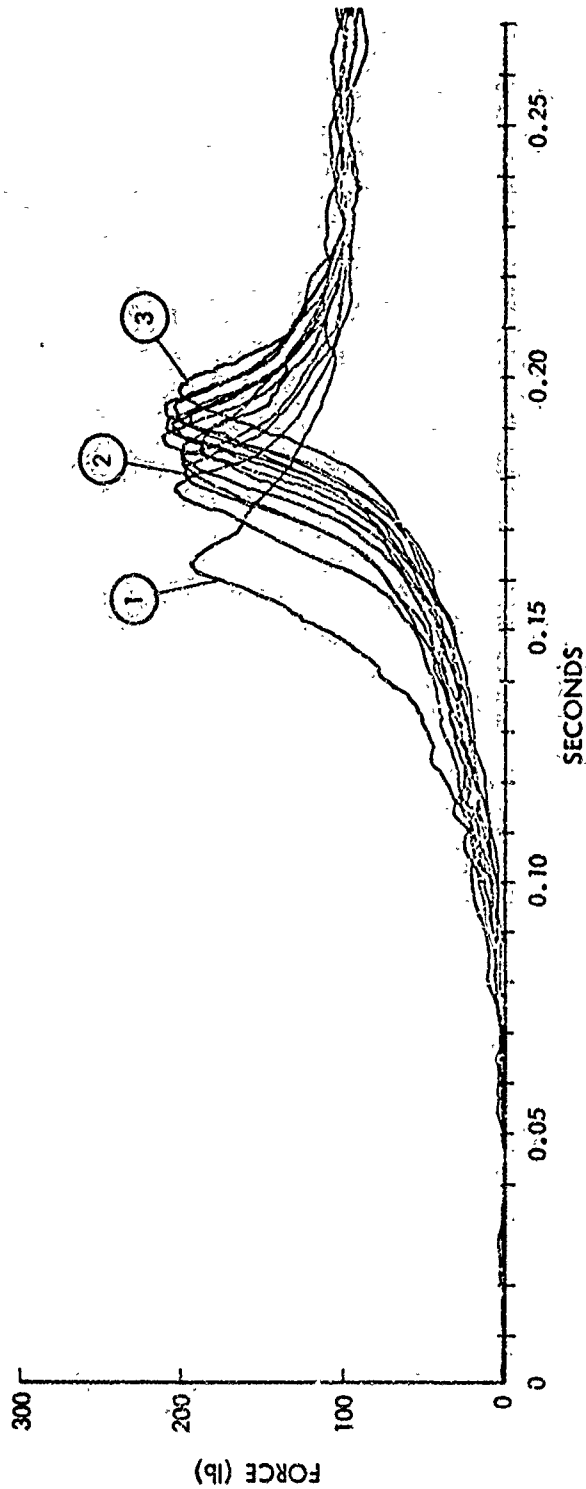
FIG. 8 OPENING FORCE OF A SOLID FLAT PRIMARY PARACHUTE

REPRODUCED FROM REFERENCE (3)
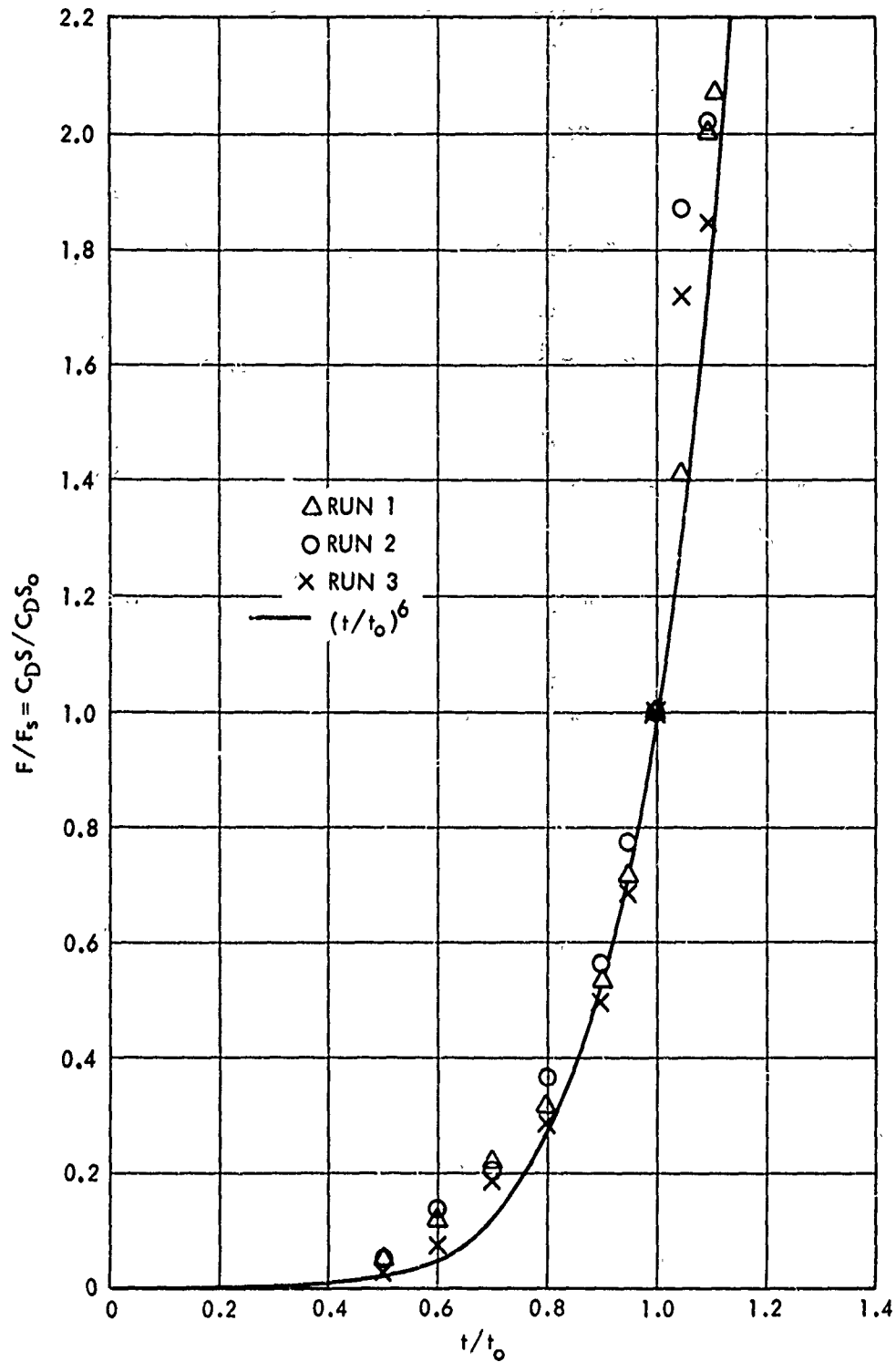
FIG. 9 REPEATABILITY OF THE SOLID, FLAT, PRIMARY PARACHUTE DRAG AREA UNDER
CONSTANT TEST CONDITIONS
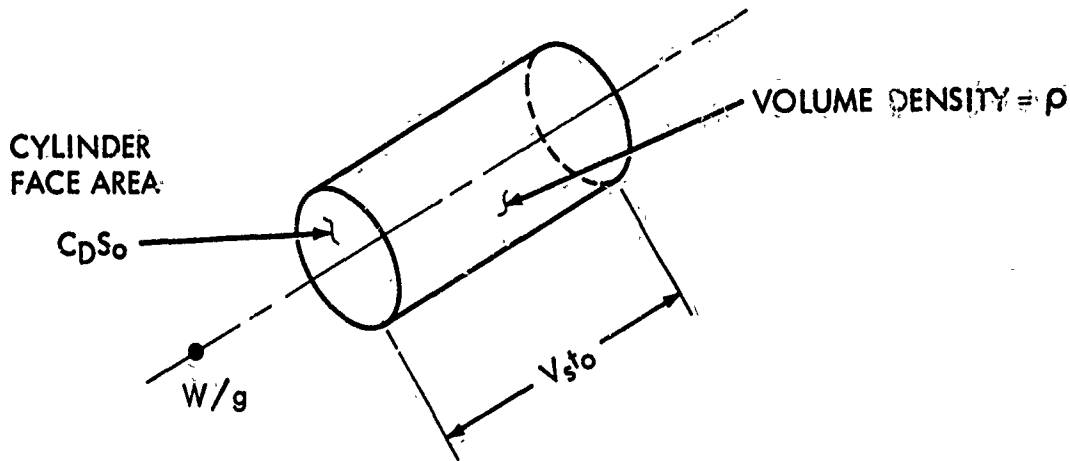
FIG. 10   VISUALIZATION OF THE MASS RATIO CONCEPT

It has been previously shown that the deployment geometry is independent of altitude and velocity. It is now demonstrated that the mass ratio (M) is the scale factor which controls the velocity and force profiles during parachute deployment.

Substituting M and $C_D S / C_D S_o$ into equation (2)

$$\frac{1}{t_o} \int_0^t \left[(1 - \eta)^2 \left(\frac{t}{t_o}\right)^6 + 2\eta (1 - \eta) \left(\frac{t}{t_o}\right)^3 + \eta^2 \right] dt = -MV_s \int_{V_s}^{V} \frac{dV}{V^2}$$

Integrating and solving for V/V_s

$$\frac{V}{V_s} = \frac{1}{1 + \frac{1}{M} \left[\frac{(1 - \eta)^2}{7} \left(\frac{t}{t_o}\right)^7 + \frac{\eta (1 - \eta)}{2} \left(\frac{t}{t_o}\right)^4 + \eta^2 \frac{t}{t_o} \right]} \qquad (7)$$

The instantaneous shock factor is defined as

$$x_i = \frac{F}{F_s} = \frac{\frac{1}{2} \rho V^2 C_D S}{\frac{1}{2} \rho V_s^2 C_D S_o}$$

If the altitude variation during deployment is small, then, the density may be considered as constant

$$x_i = \frac{C_D S}{C_D S_o} \left(\frac{V}{V_s}\right)^2$$

from equations (5) and (7)

$$x_i = \frac{(1 - \eta)^2 \left(\frac{t}{t_o}\right)^6 + 2\eta (1 - \eta) \left(\frac{t}{t_o}\right)^3 + \eta^2}{\left[1 + \frac{2}{M} \left[\frac{(1 - \eta)^2}{7} \left(\frac{t}{t_o}\right)^7 + \frac{\eta(1 - \eta)}{2} \left(\frac{t}{t_o}\right)^4 + \eta^2 \frac{t}{t_o}\right]\right]^2}$$

(8)

MAXIMUM SHOCK FORCE AND TIME OF OCCURRENCE DURING THE UNFOLDING PHASE

The time of occurrence of the maximum instantaneous shock factor (x_i) is difficult to determine for the general case. However, for $\eta = 0$, the maximum shock factor and time of occurrence is readily calculated. For $\eta = 0$

$$x_i = \frac{\left(\frac{t}{t_o}\right)^6}{\left[1 + \frac{1}{7M} \left(\frac{t}{t_o}\right)^7\right]^2}$$

Setting the derivative of x_i with respect to time equal to zero and solving for t/t_o at $x_{i\ max}$

$$\left(\frac{t}{t_o}\right)_{@ x_{i\ max}} = \left(\frac{21M}{4}\right)^{\frac{1}{7}}$$

(9)
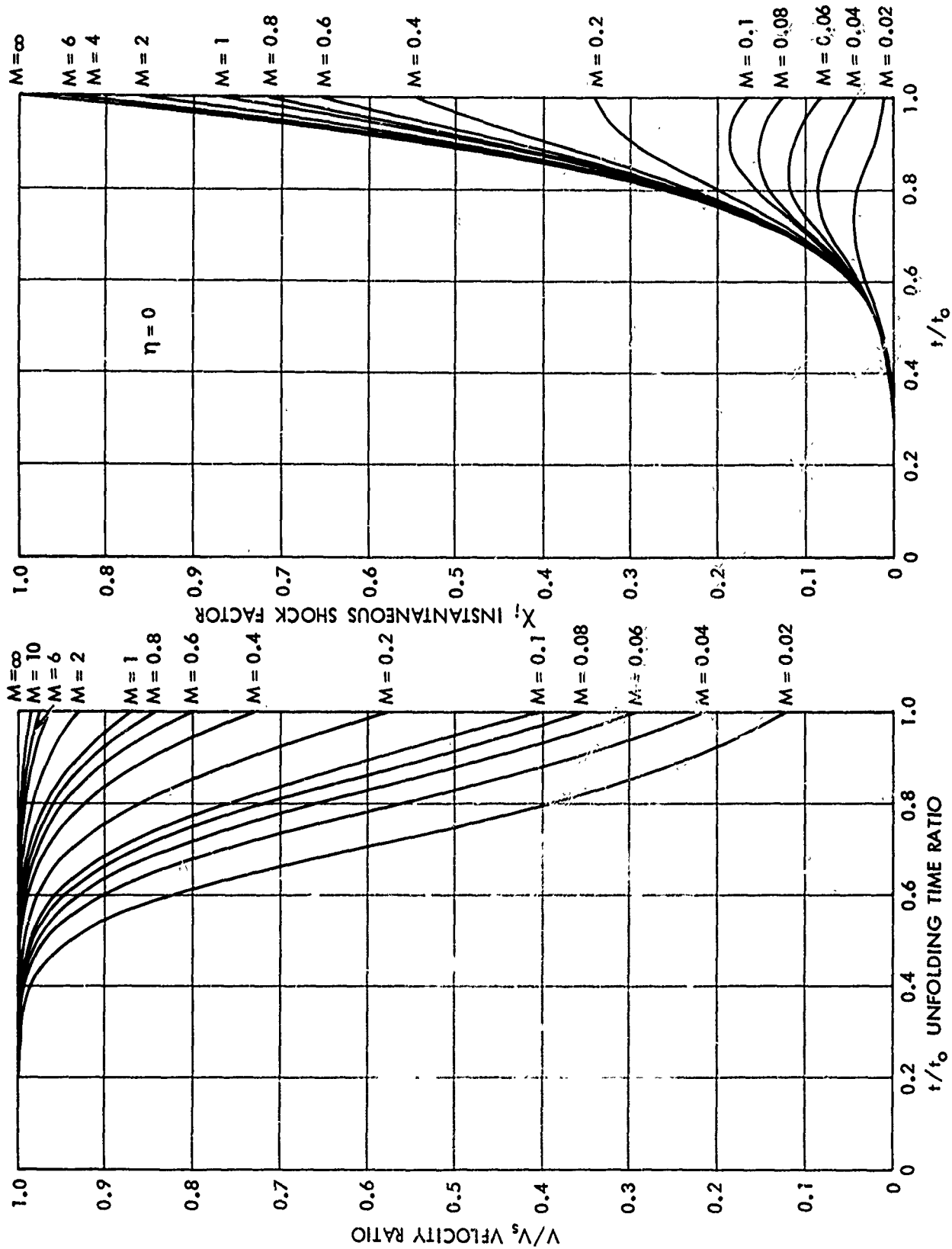
FIG. 11 EFFECT OF INITIAL AREA AND MASS RATIO ON THE SHOCK FACTOR
AND VELOCITY RATIO DURING THE UNFOLDING PHASE FOR $\eta = 0$

14
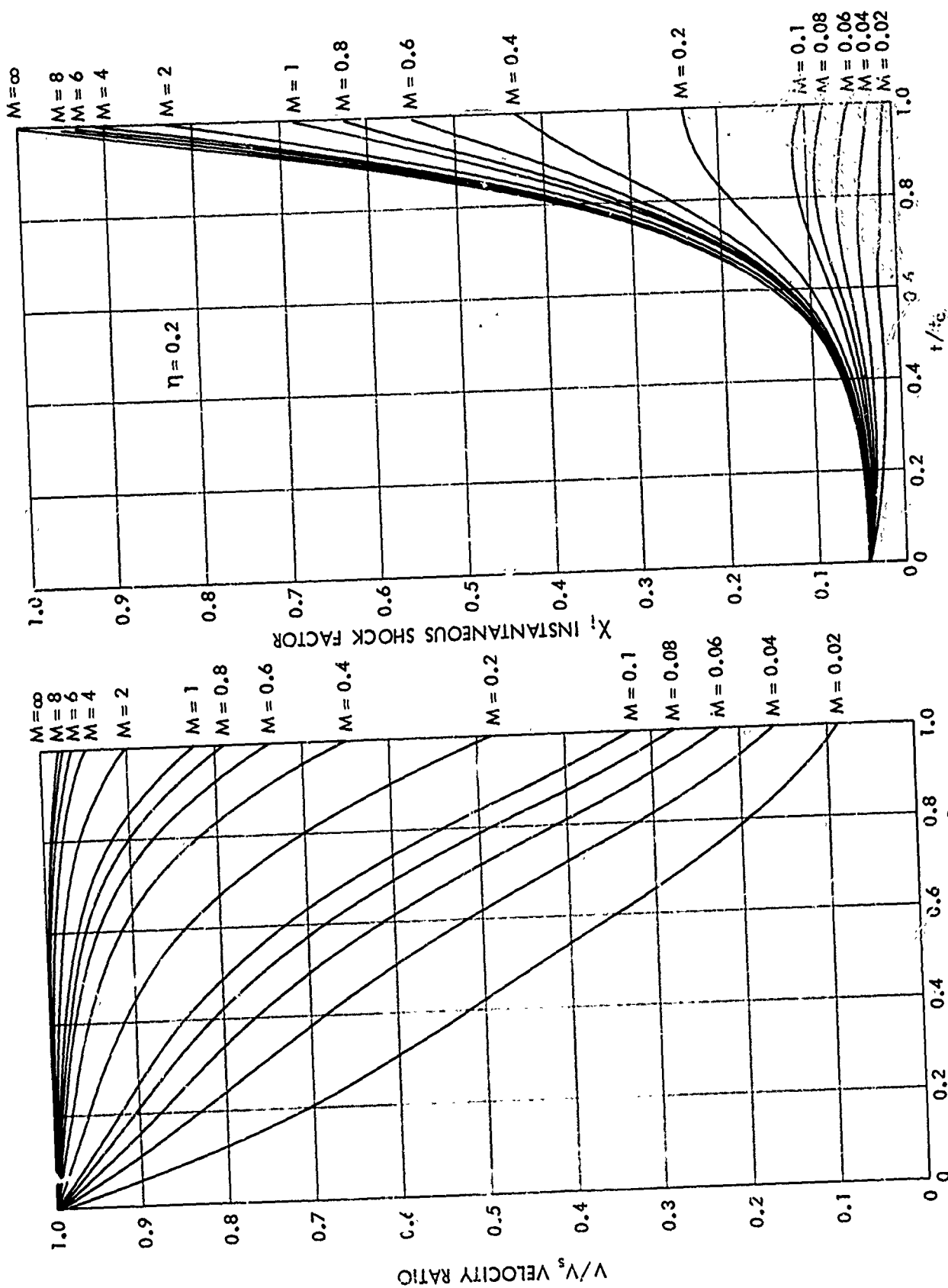
FIG. 12 EFFECT OF INITIAL AREA AND MASS RATIO ON THE SHOCK FACTOR AND VELOCITY RATIO DURING THE UNFOLDING PHASE FOR $\eta = 0.2$
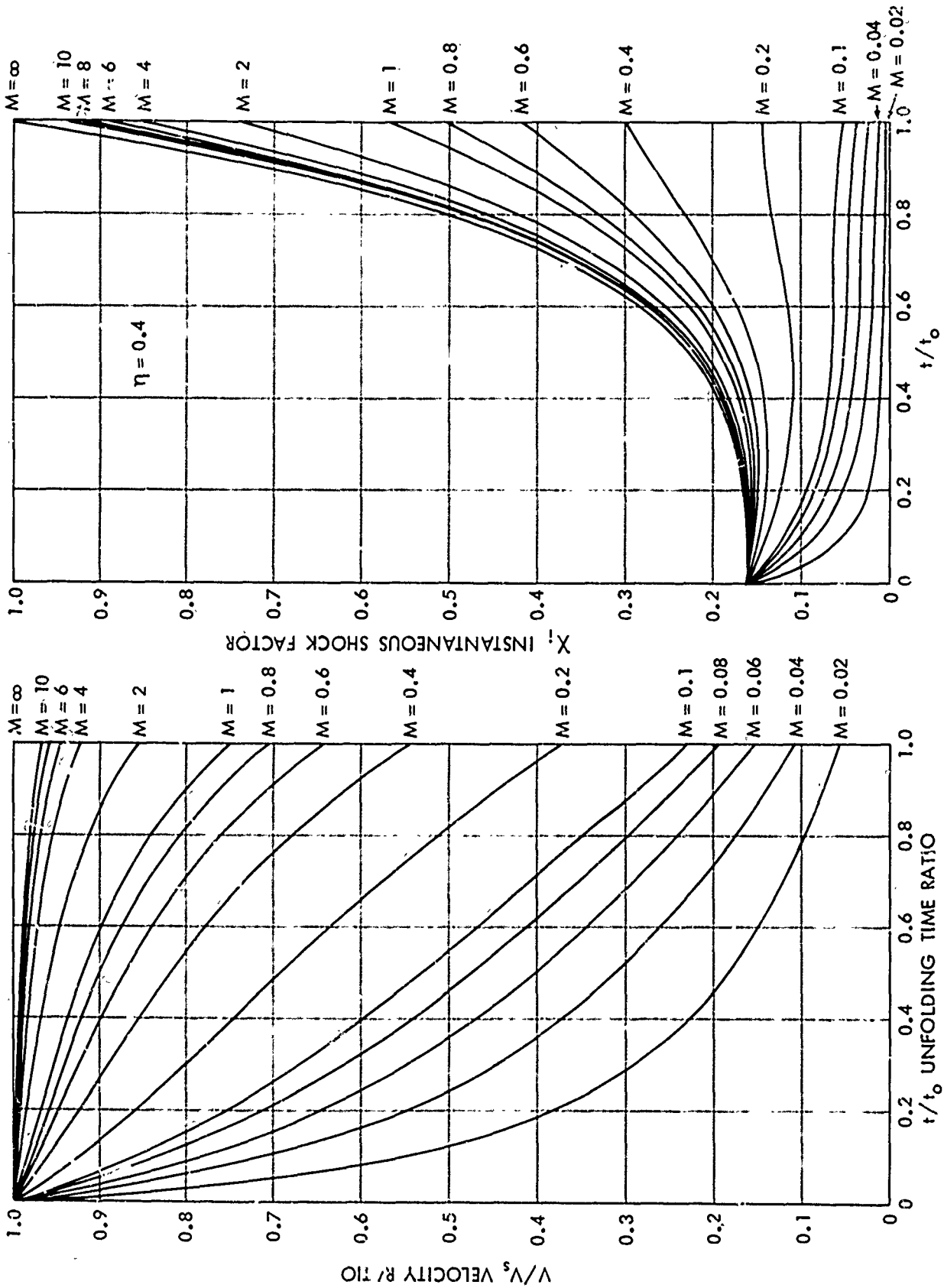
FIG. 13 EFFECT OF INITIAL AREA AND MASS RATIO ON THE SHOCK FACTOR AND VELOCITY RATIO DURING THE UNFOLDING PHASE FOR $\eta = 0.4$

and the maximum shock factor is

$$x_{i\ max} \approx \frac{16}{49}\left(\frac{21M}{4}\right)^{\frac{6}{7}} \tag{10}$$

Equations (9) and (10) are valid for values of $M \leq \frac{4}{21}$, since for larger values of M, the maximum shock force occurs in the elastic phase of inflation.

Figures 11, 12, and 13 illustrate the velocity and force profiles generated from equations (7) and (8) for initial projected area ratios of η = 0, 0.2, and 0.4, with various mass ratios.

METHODS FOR CALCULATION OF THE REFERENCE TIME (t_o)

Although the ratio concept is an ideal method to analyze the effects of the various parameters such as initial area, mass ratio, launching conditions on the velocity, and force profiles of the opening parachute, a means of calculating the reference time (t_o) is required before specific values can be computed. In order to calculate t_o, it is necessary to develop methods for computing the varying mass flow into the inflating canopy mouth and the varying mass flow out through the inflated canopy surface area. It is also necessary to define the volume of air ($\underline{V}_o$) which must be collected during the inflation process.
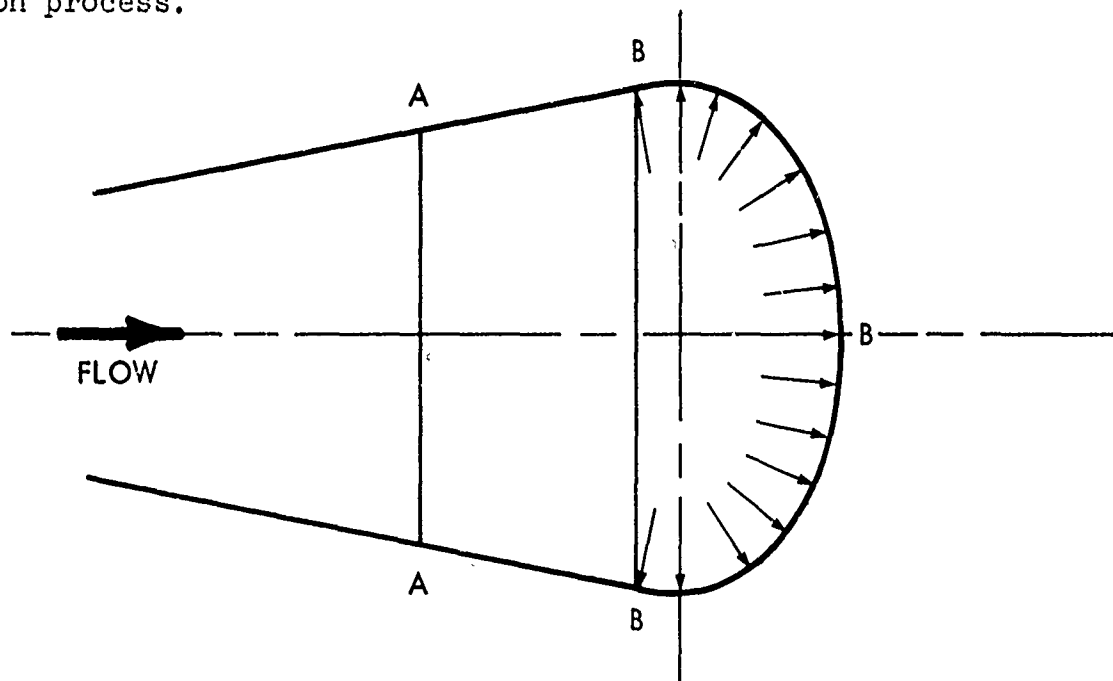
FIG. 14 PARTIALLY INFLATED PARACHUTE CANOPY

Figure 14 represents a solid cloth-type parachute canopy at some instance during inflation. At any given instance, the parachute drag area is proportional to the maximum inflated diameter. Also, the maximum diameter in conjunction with the suspension lines determines the inflow mouth area (A-A) and the pressurized canopy area (B-B-B). This observation provided the basis for the following assumptions.

a. The ratio of the instantaneous mouth inlet area to the steady-state, fully inflated mouth area is in the same ratio as the instantaneous drag area.

$$\frac{A_M}{A_{Mo}} = \frac{C_D S}{C_D S_o}$$

b. The ratio of the instantaneous pressurized cloth surface area to the canopy surface area is in the same ratio as the instantaneous drag area.

$$\frac{S}{S_o} = \frac{C_D S}{C_D S_o}$$

c. Since the suspension lines in the unpressurized area of the canopy are straight, a pressure differential has not developed, and, therefore, the net airflow in this zone is zero.

Based on the foregoing assumptions, the mass flow equation can be written

$$dm = m \text{ inflow} - m \text{ outflow}$$

$$\rho \frac{dV}{dt} = \rho V A_{Mo} \frac{C_D S}{C_D S_o} - \rho A_{So} \frac{C_D S}{C_D S_o} P \qquad (11)$$

From equation (3)

$$\frac{C_D S}{C_D S_o} = \left(\frac{t}{t_o}\right)^6 \; ; \text{ for } \eta = 0$$

18

From equation (7)

$$V = \frac{V_s}{1 + \frac{1}{7M}\left(\frac{t}{t_o}\right)^7} \quad ; \quad \text{for } \eta = 0$$

From equation (A-2)

$$P = k\left(\frac{C_p \rho}{2}\right)^n V^{2n}$$

Appendix A describes how the permeability of cloth (P) is applied to the canopy inflation problem. Appendix B describes the method for determining the volume of air $(\underline{V}_o)$ associated with the steady-state inflated canopy.

Calculation of the reference time is simplified by eliminating the effect of initial area and calculating t_o for a parachute inflating from zero drag area. A correction for the time lapse required to theoretically inflate the parachute from zero to the initial drag area of the particular problem can be determined from the drag area ratio-time relationship. Substituting into equation (11)

$$\int_0^{\underline{V}_o} d\underline{V} = A_{Mo}V_s \int_0^{t_o} \frac{\left(\frac{t}{t_o}\right)^6}{1 + \frac{1}{7M}\left(\frac{t}{t_o}\right)^7} \, dt - A_{So}k\left(\frac{C_p \rho}{2}\right)^n$$

$$\int_0^{t_o} \left(\frac{t}{t_o}\right)^6 \left[\frac{V_s}{1 + \frac{1}{7M}\left(\frac{t}{t_o}\right)^7}\right]^{2n} \, dt \qquad (12)$$

19

Measured values of the cloth permeability parameter (n) indicate a data range from 0.57403 through 0.63246. A convenient solution to the reference time equation evolves when n is assigned a value of 1/2. Integrating equation (12) and using

$$V_s t_o M = \frac{2W}{g\rho C_D S_o}$$

$$t_o = \frac{14W}{g\rho V_s C_D S_o} \left[e^{\frac{g\rho V_o}{2W} \left[\frac{C_D S_o}{A_{Mo} - A_{So} k \left(\frac{C_p \rho}{2} \right)^{1/2}} \right]} - 1 \right] \quad (13)$$

Equation (13) expresses the unfolding reference time (t_o) in terms of mass, altitude, snatch velocity, airflow characteristics of the cloth and the steady-state parachute geometry. Note that the term $g\rho V_o/W$ is the ratio of the included air mass to the mass of the retarded hardware. Multiplying both sides of equation (13) by V_s demonstrates that

$$V_s t_o = \text{a constant which is a function of altitude}$$

The effect of altitude on the unfolding reference time (t_o) of a T-10 type parachute, based on equation (13), at constant velocity and constant dynamic pressure is to decrease as the altitude rises, Figure 15. In the rarefied atmosphere at altitudes above 75,000 feet, the reference time tends to become constant. The unfolding distance, Figure 16, is the same for both modes of operation.

An unknown factor in this study is the magnitude and the variation of the pressure coefficient on an actual canopy during deployment. A pressure coefficient of 1.15 has been assumed.

Integration of equation (12) for a realistic value of n yields a more accurate value of t_o in the lower altitude region of deployment. In the higher altitude region where the canopy cloth is relatively imporous, the values of t_o obtained from equations (13) and (14) are nearly equal. The opening-shock force is strongly influenced by the inflation time. Because of this, the value of t_o determined by equation (14) should be used. However, since the reference time (t_o)
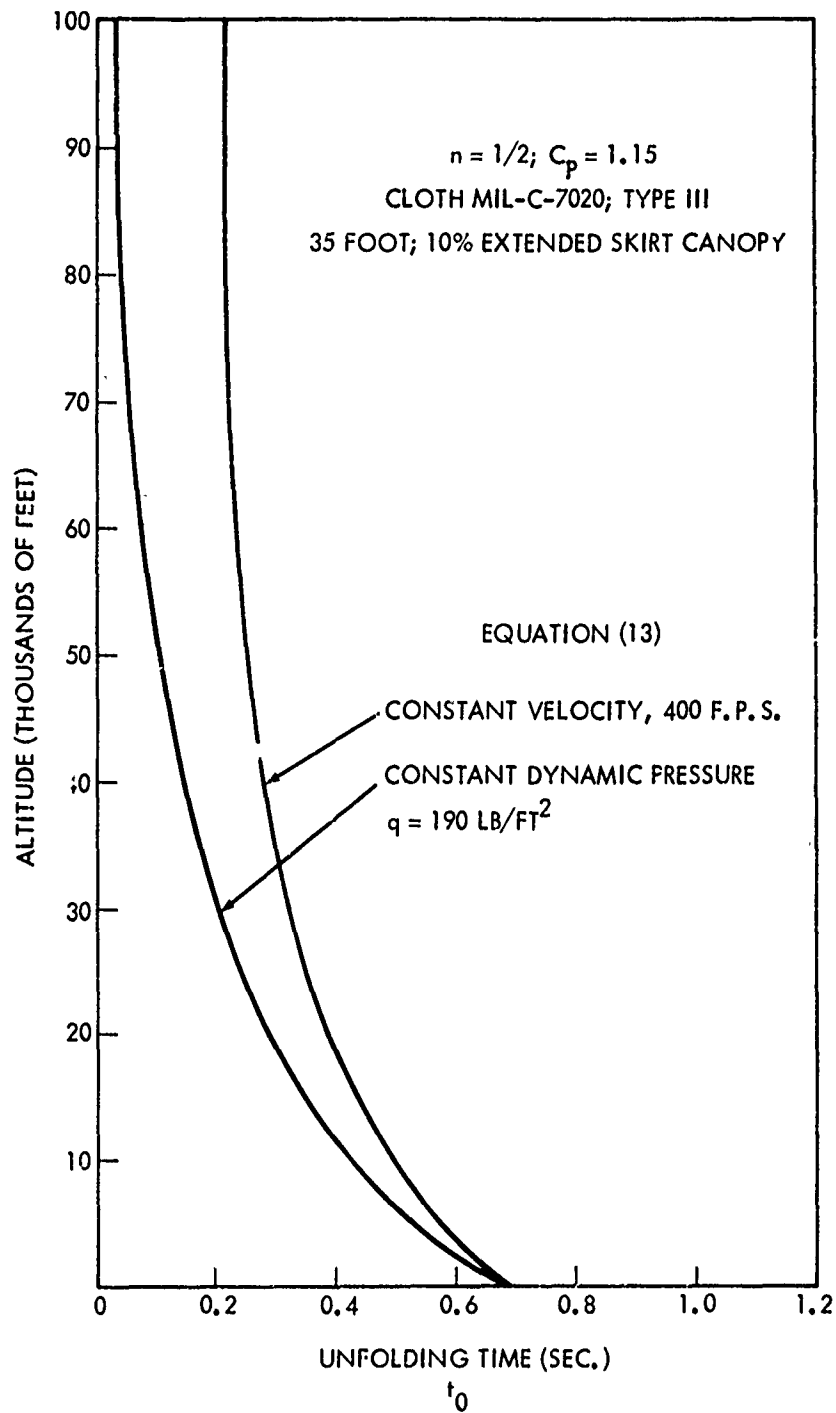
$$n = 1/2; \quad C_p = 1.15$$

CLOTH MIL-C-7020; TYPE III

35 FOOT; 10% EXTENDED SKIRT CANOPY

EQUATION (13)

CONSTANT VELOCITY, 400 F.P.S.

CONSTANT DYNAMIC PRESSURE

$$q = 190 \text{ LB/FT}^2$$

ALTITUDE (THOUSANDS OF FEET)

UNFOLDING TIME (SEC.)

t_0

FIG. 15 EFFECT OF ALTITUDE ON THE UNFOLDING TIME
"t_o" AT CONSTANT VELOCITY AND CONSTANT
DYNAMIC PRESSURE FOR n = 1/2

$n = 1/2;\ C_p = 1.15$

CLOTH MIL-C-7020; TYPE III

35 FOOT; 10% EXTENDED SKIRT CANOPY

EQUATION (13)

CONSTANT VELOCITY = 400 F.P.S.

CONSTANT DYNAMIC PRESSURE
$q = 190\ LB/FT$

ALTITUDE (THOUSANDS OF FEET)

UNFOLDING DISTANCE (FEET)
$V_s t_o$

FIG. 16 EFFECT OF ALTITUDE ON THE UNFOLDING DISTANCE
AT CONSTANT VELOCITY AND CONSTANT DYNAMIC
PRESSURE FOR $n = 1/2$

determined from equation (13) is always less than the t_o calculated from equation (14), it can therefore be used to estimate values for use in equation (14). (See Figures 17 and 18.)

$$\underline{V}_o = A_{Mo}V_s t_o M \ln \left[1 + \frac{1}{7M} \right] - A_{So} k \left(\frac{C_P}{2} \right)^n$$

$$\int_o^{t_o} \left(\frac{t}{t_o} \right)^6 \left[\frac{V_s}{1 + \frac{1}{7M}\left(\frac{t}{t_o}\right)^7} \right]^{2n} \cdot dt \qquad (14)$$

CORRECTION OF t_o FOR INITIAL AREA EFFECTS

The unfolding reference time (t_o) calculated by the previous methods assumes that the parachute inflates from zero drag area. In reality, a parachute has a drag area at the beginning of inflation. Once t_o has been calculated, a correction can be applied, based upon what is known about the initial conditions.

Case A - When the initial projected area is known

$$\frac{A_i}{A_c} = \left(\frac{t_i}{t_o} \right)^3$$

$$t_i = \left(\frac{A_i}{A_c} \right)^{1/3} t_o \text{ calculated}$$

$$t_o \text{ corrected} = \left[1 - \left(\frac{A_i}{A_c} \right)^{1/3} \right] t_o \text{ calculated} \qquad (15)$$
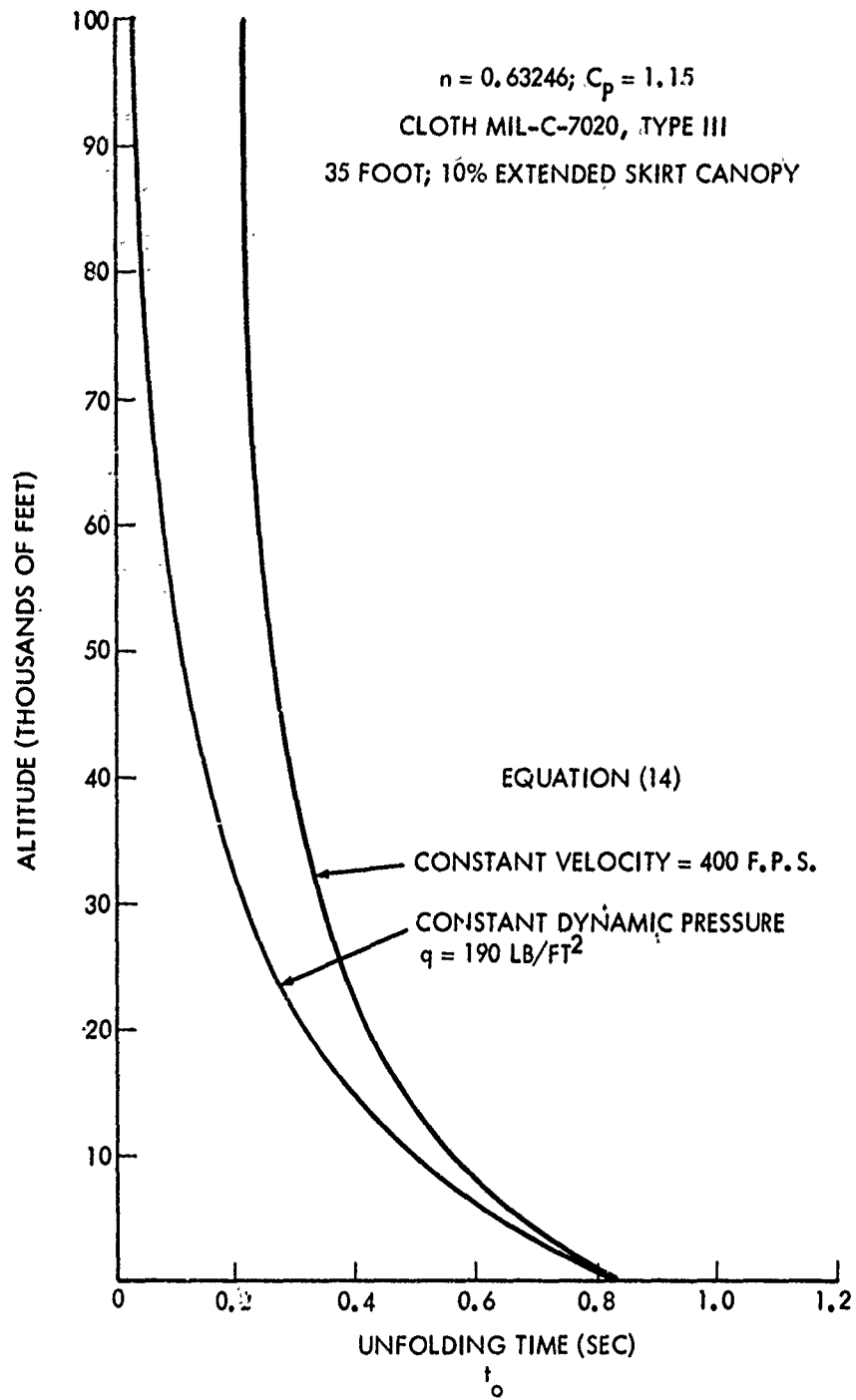
23

$n = 0.63246; \; C_p = 1.15$

CLOTH MIL-C-7020, TYPE III

35 FOOT; 10% EXTENDED SKIRT CANOPY

EQUATION (14)

CONSTANT VELOCITY = 400 F.P.S.

CONSTANT DYNAMIC PRESSURE
$q = 190 \; LB/FT^2$

ALTITUDE (THOUSANDS OF FEET)

UNFOLDING TIME (SEC)

t_o

FIG. 17 EFFECT OF ALTITUDE ON THE UNFOLDING TIME "t_o" AT
CONSTANT VELOCITY AND CONSTANT DYNAMIC PRESSURE
FOR $n = 0.63246$

$n = 0.63246;\ C_p = 1.15$
CLOTH MIL-C-7020, TYPE III
35 FOOT; 10% EXTENDED SKIRT CANOPY

EQUATION (14)

CONSTANT VELOCITY = 400 F.P.S.

CONSTANT DYNAMIC PRESSURE
$q = 190\ LB/FT^2$
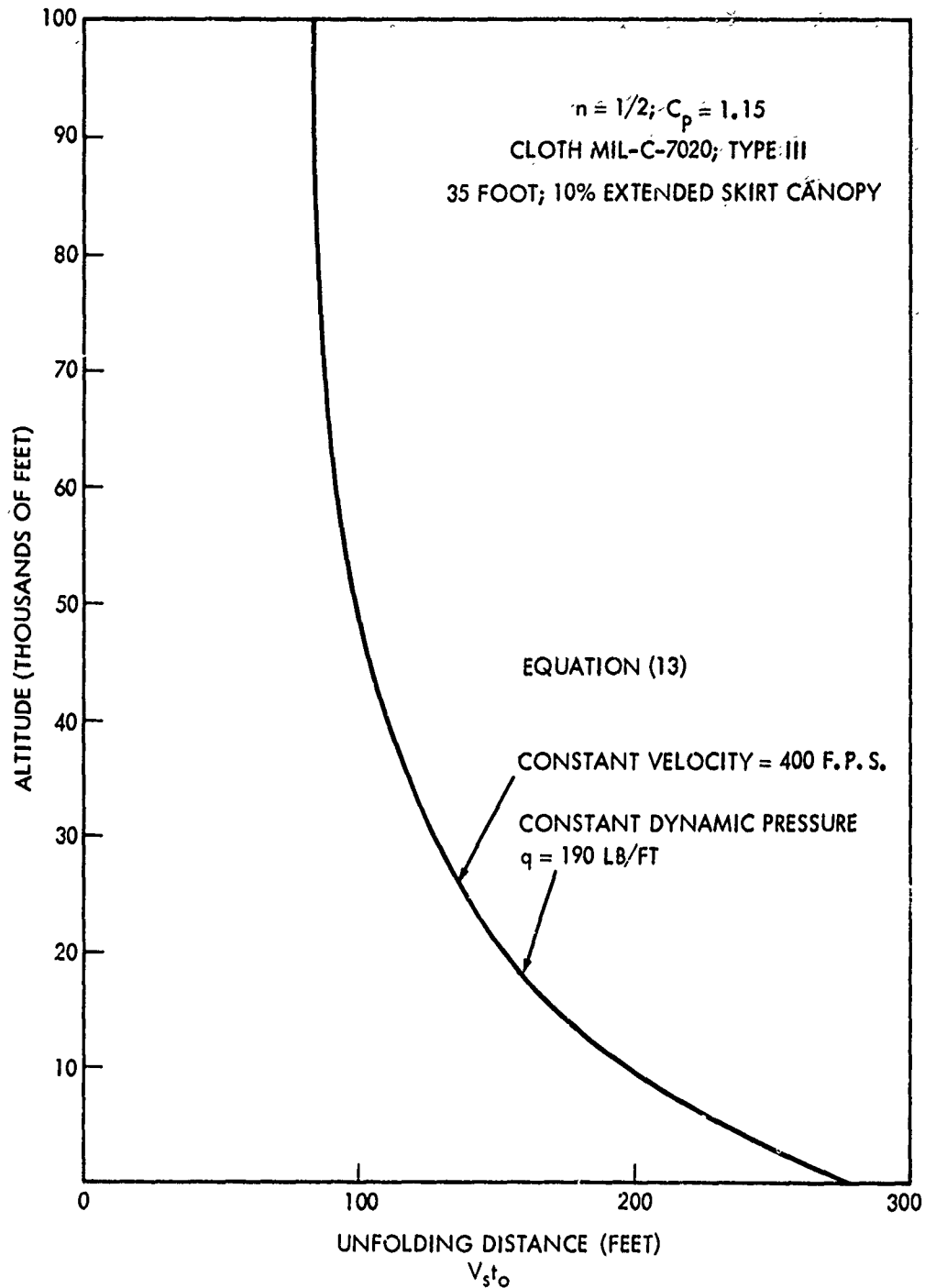
ALTITUDE (THOUSANDS OF FEET)

UNFOLDING DISTANCE (FEET)
$V_s t_o$
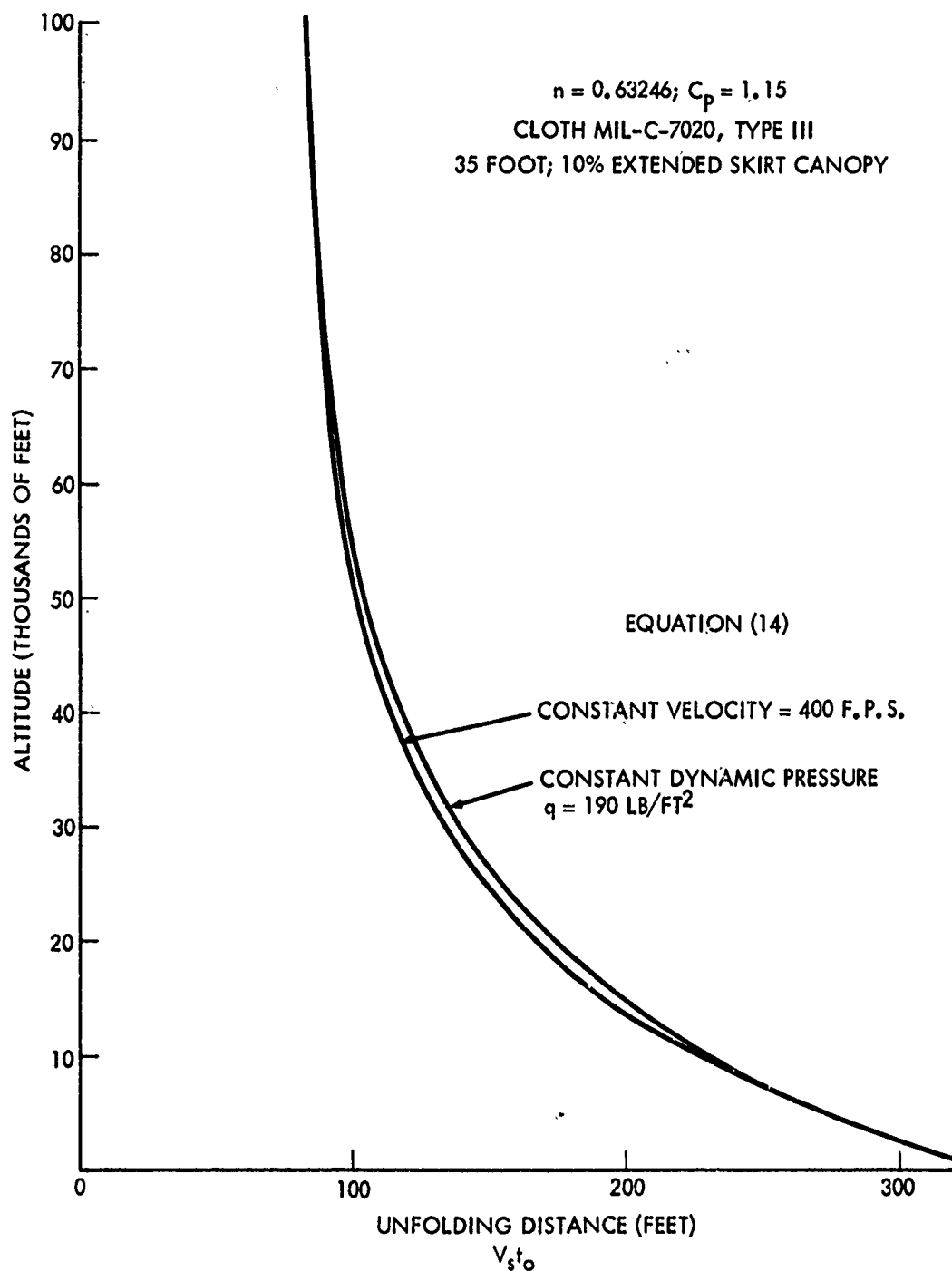
FIG. 18 EFFECT OF ALTITUDE ON THE UNFOLDING DISTANCE AT
CONSTANT VELOCITY AND CONSTANT DYNAMIC PRESSURE
FOR $n = 0.63246$

where A_c is the projected area of the fully inflated canopy based on the maximum inflated diameter.

Case B - When the initial drag area is known

$$\frac{c_D S_i}{c_D S_o} = \left(\frac{t_i}{t_o}\right)^6$$

$$t_i = \left(\frac{c_D S_i}{c_D S_o}\right)^{1/6} t_o \text{ calculated}$$

$$t_o \text{ corrected} = \left[1 - \left(\frac{c_D S_i}{c_D S_o}\right)^{1/6}\right] t_o \text{ calculated} \qquad (16)$$

The mass ratio should now be adjusted for the corrected t_o before velocity and force profiles are determined.

As an example of this method of opening-shock analysis, let us examine the effect of altitude on the opening-shock force of a T-10 type parachute retarding a 200-pound weight from a snatch velocity of $V_s = 400$ feet per second at sea level. Conditions of constant velocity and constant dynamic pressure are investigated. The results are presented in Figure (19). At low altitudes, the opening-shock force is less than the steady-state drag force; however, as altitude rises, the opening shock eventually exceeds the steady-state drag force at some altitude. This trend is in agreement with field test observations.

OPENING-SHOCK FORCE, VELOCITY RATIO, AND INFLATION TIME DURING THE ELASTIC PHASE OF PARACHUTE INFLATION

The mass ratio (M) is an important parameter in parachute analysis. For values of $M \ll 4/21$, the maximum opening-shock force occurs early in the inflation process, and the elastic properties of the canopy are not significant. As the mass ratio approaches $M = 4/21$, the magnitude of the opening-shock force increases, and the time of occurrence happens later in the deployment sequence. For mass ratios $M > 4/21$, the maximum shock force will occur after the reference time (t_o). Parachutes designed for high mass ratio operation must provide a structure of sufficient constructed strength (F_c) so that
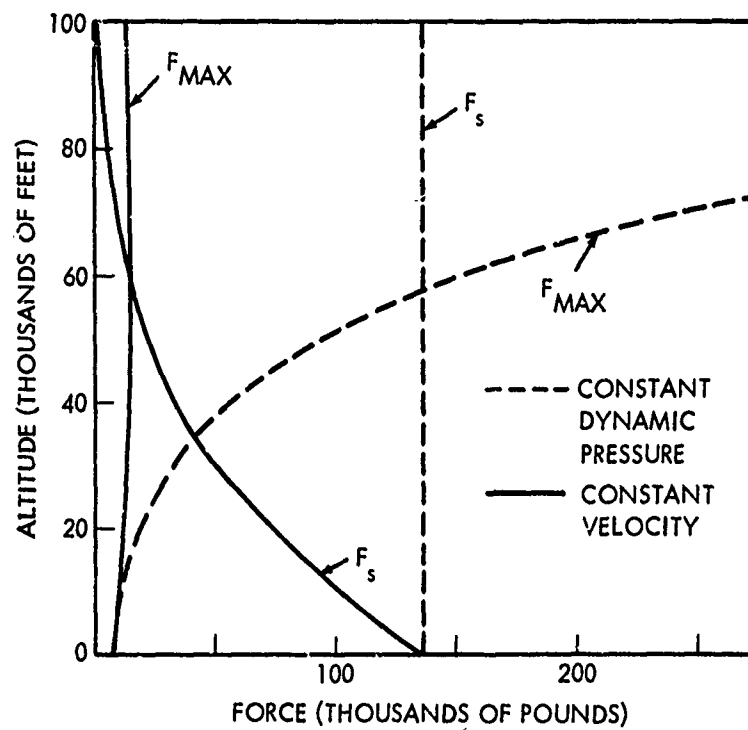
FIG. 19 VARIATION OF STEADY-STATE DRAG, F_s, AND MAXIMUM OPENING
SHOCK WITH ALTITUDE FOR CONSTANT VELOCITY AND CONSTANT
DYNAMIC PRESSURE

the actual elongation of the canopy under load is less than the maximum extensibility (ε_{max}) of the materials.

Development of the analysis in the elastic phase of inflation is similar to the technique used in the unfolding phase. Newton's second law of motion is used, together with the drag area ratio signature,

$$\frac{c_D S}{c_D S_o} = \left(\frac{t}{t_o}\right)^6$$

which is still valid as shown in Figures 7 and 9, and mass ratio.

$$\frac{1}{Mt_o} \int_{t_o}^{t} \left(\frac{t}{t_o}\right)^6 dt = V_s \int_{V_o}^{V} \frac{-dV}{V^2}$$

Integrating and solving for $\dfrac{V}{V_s}$

$$\frac{V}{V_s} = \frac{1}{\dfrac{V_s}{V_o} + \dfrac{1}{7M}\left[\left(\dfrac{t}{t_o}\right)^7 - 1\right]} \tag{17}$$

where $\dfrac{V_o}{V_s}$ is the velocity ratio of the unfolding process at time $t = t_o$, equation (7).

$$\frac{V_o}{V_s} = \frac{1}{1 + \dfrac{1}{M}\left[\dfrac{(1-\eta)^2}{7} + \dfrac{\eta(1-\eta)}{2} + \eta^2\right]} \tag{18}$$

For convenience, let $K = \dfrac{V_o}{V_s}$

The instantaneous shock factor in the elastic phase becomes

$$x_i = \frac{C_D S}{C_D S_o} \left(\frac{V}{V_s}\right)^2$$

$$x_i = \frac{\left(\dfrac{t}{t_o}\right)^6}{\left[\dfrac{1}{K} + \dfrac{1}{7M}\left[\left(\dfrac{t}{t_o}\right)^7 - 1\right]\right]^2} \tag{19}$$

The end point of the inflation process depends upon the applied loads, elasticity of the canopy, and the constructed strength of the parachute. A linear load elongation relationship is utilized to determine the maximum drag area.

$$\frac{\epsilon}{F} = \frac{\epsilon_{max}}{F_c}$$

$$\epsilon = \frac{F \, \epsilon_{max}}{F_c} \tag{20}$$

The force (F) is initially the instantaneous force at the end of the unfolding process

$$F = X_o F_s \tag{21}$$

where X_o is the shock factor of the unfolding phase at $t = t_o$

$$X_o = \frac{(1 - \eta)^2 + 2\eta(1 - \eta) + \eta^2}{\left[1 + \frac{1}{M} \left[\frac{(1 - \eta)^2}{7} + \frac{\eta(1 - \eta)}{2} + \eta^2 \right] \right]^2} \tag{22}$$

Since the inflated shape is defined, the drag coefficient is considered to be constant, and the instantaneous force is proportional to the dynamic pressure and projected area. The maximum projected area would be developed if the dynamic pressure remained constant during the elastic phase. Under very high mass ratios, this is nearly the case over this very brief time period; but as the mass ratio decreases, the velocity decay has a more significant effect. The simplest approach for all mass ratios is to determine the maximum drag area of the canopy as if elastic inflation had occurred at constant dynamic pressure. Then utilizing the time ratio determined as an end point, intermediate shock factors can be calculated from equation (19) and the maximum force assessed.

The following technique for determining the maximum drag area was derived from a method first suggested by Mr. J. F. McNelia of the Naval Ordnance Laboratory (NOL). The initial force ($X_o F_s$) causes the canopy to increase in projected area. The new projected area in turn increases the total force on the canopy which produces a secondary projected area increase. The resulting series of events are resisted by the parachute materials. If the parachute has sufficient constructed strength, the series converges to a limiting value. Insufficient constructed strength results in a series that diverges, indicating failures. Combining equation (20) and (21), let

$$\epsilon_o = \frac{X_o F_s}{F_c} \epsilon_{max} \tag{23}$$

The next force in the series at constant c

$$F_1 = X_o F_s \frac{A_1}{A_c}$$

where

$$\frac{A_1}{A_c} = (1 + \epsilon_o)^2$$

$$F_1 = X_o F_s (1 + \epsilon_o)^2 \qquad (24)$$

and the elongation produced by this force

$$\epsilon_1 = \frac{F_1}{F_c} \epsilon_{max} = \frac{X_o F_s}{F_c} \epsilon_{max} (1 + \epsilon_o)^2 \qquad (25)$$

$$\epsilon_1 = \frac{X_o F_s}{F_c} \epsilon_{max} \left(1 + \frac{X_o F_s}{F_c} \epsilon_{max}\right)^2 \qquad (26)$$

$$\epsilon_1 = \epsilon_o (1 + \epsilon_o)^2 \qquad (27)$$

produces another force

$$F_2 = X_o F_s (1 + \epsilon_1)^2 \qquad (28)$$

and the next elongation

$$\epsilon_2 = \frac{F_2}{F_c} \epsilon_{max} = \frac{X_o F_s}{F_c} (1 + \epsilon_1)^2 \epsilon_{max} \qquad (29)$$

$$\epsilon_2 = \frac{X_o F_s}{F_c} \epsilon_{max} \left[1 + \frac{X_o F_s}{F_c} \epsilon_{max} \left(1 + \frac{X_o F_s}{F_c} \epsilon_{max}\right)^2\right]^2 \qquad (30)$$

$$\epsilon_2 = \epsilon_o (1 + \epsilon_o (1 + \epsilon_o)^2)^2 \qquad (31)$$

The series is further expanded until a convergent or divergent character is ascertained. If the series diverges, the constructed strength (F_c) must be increased and the series recalculated.

An advantage of this system is that the required canopy constructed strength can be determined for a given set of deployment conditions. The limiting value of the series (ϵ_ℓ) determines the end point time ratio.

$$\left(\frac{t}{t_0}\right)^6 = \frac{C_D S_{max}}{C_D S_0} = (1 + \epsilon_\ell)^2$$

$$\left(\frac{t}{t_0}\right) = \left(\frac{C_D S_{max}}{C_D S_0}\right)^{1/6} = (1 + \epsilon_\ell)^{1/3} \qquad (32)$$

All convergent series can be expressed in terms of ϵ_0. This relationship is shown in Figure 20 wherein the maximum drag area ratios are plotted as a function of ϵ_0.

$$\epsilon_0 = \frac{X_0 F_s}{F_c} \epsilon_{max}$$
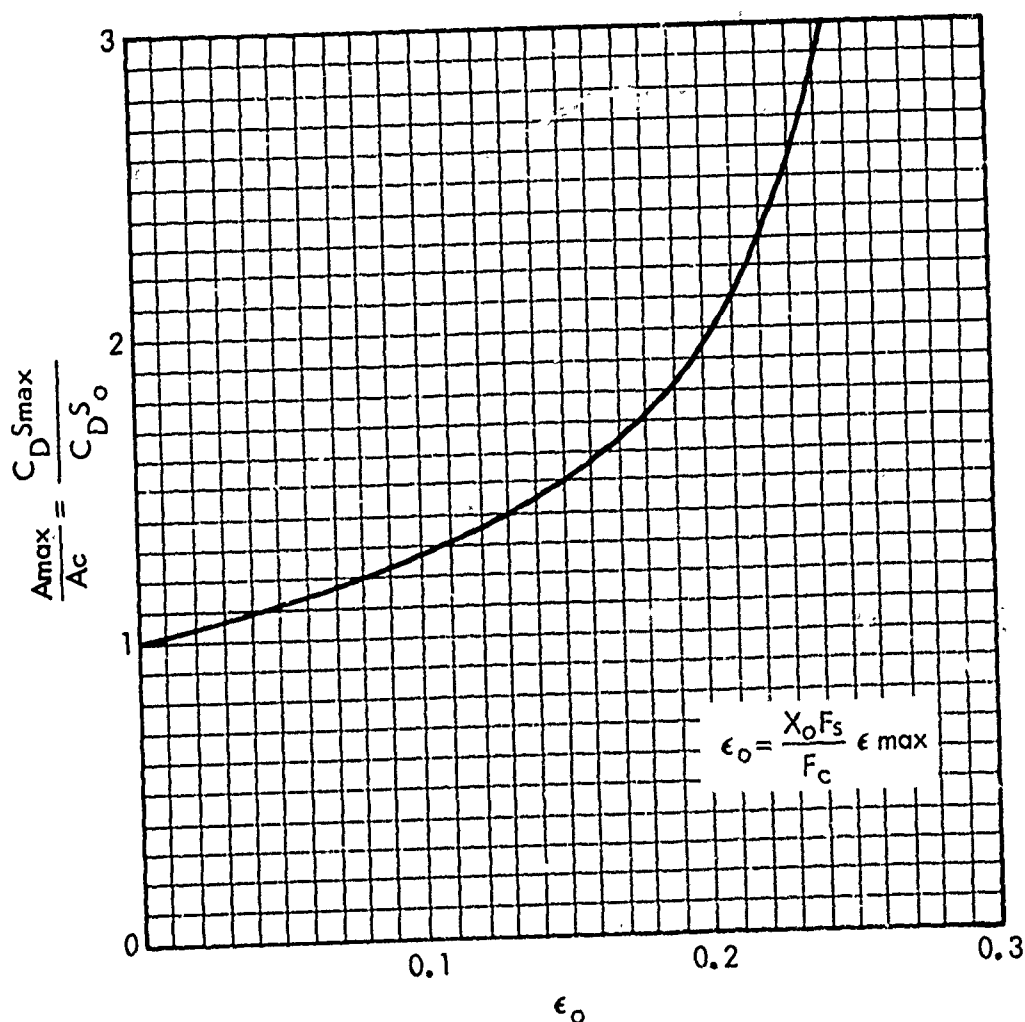
FIG. 20   MAXIMUM DRAG AREA RATIO vs INITIAL ELONGATION

The maximum sh .k factor and the time ratio at the time of occurrence of the maximum shock factor are assessed by means of equation (19) for various intermediate values between $t/t_o = 1$ and t/t_o from equation (32) using the particular mass ratio under investigation. The maximum shock force

$$F_{max} = F_s X_{i\ max} \qquad (33)$$

The time of occurrence of the maximum shock force coincides with the maximum physical size of the parachute and, therefore, is defined as the inflation time (t_f).

Examination of Figure 20 would seem to indicate that low elongation materials are desirable for parachutes operating under infinite mass. This is correct insofar as overloading is related to material elasticity.

The presented formulation, however, has not considered the inertial forces imposed upon the structure during deployment. While these forces are not studied in this report, it seems reasonable that material extensibility reduces the inertia forces in the joints and seams. In view of these two effects, an optimum material elongation should exist which maintains low inertia forces and limits parachute loading from canopy enlargement.

An illustrative problem is presented to demonstrate the effects of the elasticity of parachute materials and parachute constructed strength on opening-shock force. Example: A solid cloth parachute system is operating at a mass ratio of $M = 100$. The maximum material elongation ($\epsilon_{max} = 0.25$) and the ratio of the constructed strength to steady-state drag ($F_c/F_s = 1.75$). Assume $\eta = 0$. Find:

a. Ratio of t_f/t_o

b. Maximum shock factor $(x_{i\ max})$

c. Parachute safety factor (F_c/F_{max})

d. Determine the effect of varying the parachute constructed strength on the maximum shock factor

For mass ratios of $M > 4/21$, the maximum opening shock occurs in the elastic phase of inflation.

a. Solution for t_f/t_o, for $\eta = 0$

From equation (22)

$$X_o = \frac{1}{\left[1 + \frac{1}{7M}\right]^2}$$

$$X_o = \frac{1}{\left[1 + \frac{1}{7 \times 100}\right]^2}$$

$$X_o = .9803$$

and from equation (23)

$$\epsilon_o = X_o \frac{F_s}{F_c} \epsilon_{max}$$

$$\epsilon_o = \frac{.9803 \times .25}{1.75}$$

$$\epsilon_o = .1400$$

From Figure 20, the maximum drag area ratio

$$\frac{C_D S_{max}}{C_D S_o} = 1.45$$

The maximum time ratio (t_f/t_o)

From equation (32)

$$\frac{t_f}{t_o} = \left(\frac{C_D S_{max}}{C_D S_o}\right)^{1/6}$$

34

$$\frac{t_f}{t_o} = (1.45)^{1/6}$$

$$\frac{t_f}{t_o} = 1.064$$

b. Solution for $x_{i\ max}$

The velocity ratio at $t = t_o$ for $\eta = 0$

From equation (18)

$$\frac{V_o}{V_s} = \frac{1}{1 + \dfrac{1}{7M}}$$

$$\frac{V_o}{V_s} = \frac{1}{1 + \dfrac{1}{7 \times 100}}$$

$$\frac{V_o}{V_s} = K \doteq .9901$$

The maximum shock factor $(x_{i\ max})$

From equation (19)

$$x_{i\ max} = \frac{\left(\dfrac{t_f}{t_o}\right)^6}{\left[\dfrac{1}{K} + \dfrac{1}{7M}\left[\left(\dfrac{t_f}{t_o}\right)^7 - 1\right]\right]^2}$$

$$x_{i\ max} = \frac{(1.064)^6}{\left[\dfrac{1}{.9901} + \dfrac{1}{7(100)}\left(1.064^7 - 1\right)\right]^2}$$

$$x_{i\ max} = 1.42$$

The maximum shock force (F_{max})

From equation (33)

$$F_{max} = X_{i\ max}\ F_s$$

c.   The parachute safety factor (S.F.)

$$S.F. = \frac{F_c}{F_{max}}$$

$$x_{i\ max} = \frac{F_{max}}{F_s}\ \ \frac{F_c}{F_c} = \frac{F_{max}}{F_c}\ \ \frac{F_c}{F_s}$$

$$\frac{F_c}{F_{max}} = \frac{F_c}{F_s X_{i\ max}}$$

$$\frac{F_c}{F_{max}} = \frac{1.75}{1.42}$$

S.F. = 1.23

d. The effects of varying the parachute constructed strength can be determined by repeating the previous series of calculations for various ratios of F_c/F_s. The results are illustrated in Figure 21.
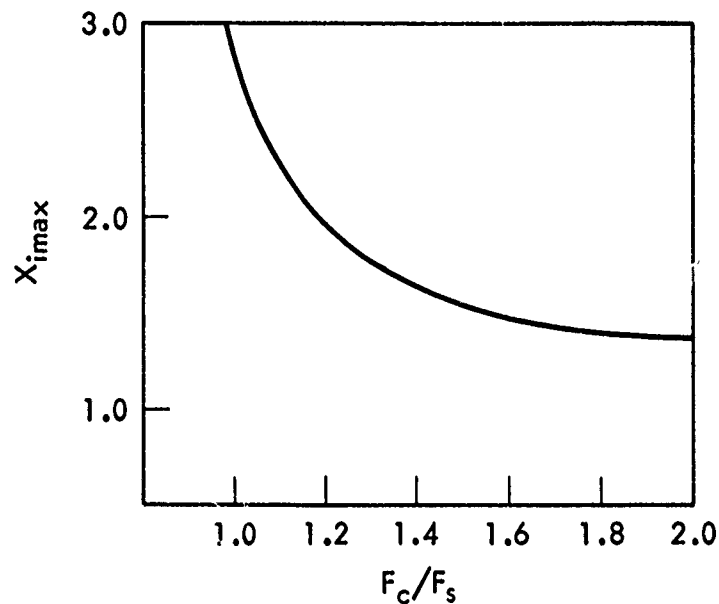
FIG. 21   EFFECT OF PARACHUTE CONSTRUCTED STRENGTH ON THE MAXIMUM SHOCK FACTOR AT CONSTANT DEPLOYMENT CONDITIONS

REFERENCES

(1) "A Method to Reduce Parachute Inflation Time with a Minor Increase in Opening Force," WADD Report TR 60-761

(2) Berndt, R. J., and DeWesse, J. H., "Filling Time Prediction Approach for Solid Cloth Type Parachute Canopies," AIAA Aerodynamic Deceleration Systems Conference, Houston, Texas 7-9 Sep 1966

(3) "Theoretical Parachute Investigations," Progress Report No. 4, Project No. 5, WADC Contract AF33 (616)-3955, University of Minnesota

(4) "Performance of and Design Criteria for Deployable Aerodynamic Decelerators," TR ASK-TR-61-579, AFFDL, AIRFORCESYSCOM, Dec 1963

(5) "Investigation of Stability of Parachutes and Development of Stable Parachutes from Fabric of Normal Porosity," Count Zeppelin Research Institute Report No. 300, 23 Mar 1943

(6) Ludtke, W. P., "A New Approach to the Determination of the Steady-State Inflated Shape and Included Volume of Several Parachute Types," NOLTR 69-159, 11 Sep 1969

(7) Ludtke, W. P., "A New Approach to the Determination of the Steady-State Inflated Shape and Included Volume of Several Parachute Types in 24-Gore and 30-Gore Configurations," NOLTR 70-178, 3 Sep 1970

APPENDIX A

APPLICATION OF CLOTH PERMEABILITY TO THE CALCULATION OF
THE INFLATION TIME OF SOLID CLOTH PARACHUTES

The mass outflow through the pressurized region of an inflating
solid cloth parachute at any instant is dependent upon the canopy
area which is subjected to airflow and the rate of airflow through
that area. The variation of pressurized area as a function of
reference time (t_o) was earlier assumed to be proportional to the
instantaneous drag area ratio, leaving only the rate of airflow
problem to solve. The permeability parameter of cloth was a natural
choice for determining the rate of airflow through the cloth as a
function of pressure differential across the cloth. Heretofore,
these data have been more of a qualitative, rather than quantitative,
value. A new method of analysis was developed wherein a generalized
curve of the form $P = k(\Delta P)^n$ was fitted to cloth permeability data
for a number of different cloths and gives surprisingly good agree-
ment over the pressure differential range of available data. The
pressure differential was then related to the trajectory conditions
to give a generalized expression which can be used in the finite
mass ratio range, as well as the infinite mass case. The perme-
ability properties were transformed into a mass flow ratio, M',
which shows agreement with the effective porosity concept.

Measured and calculated permeability-pressure data for several
standard cloths are illustrated in Figure A-1. This method has
been applied to various types of cloth between the extremes of a
highly permeable 3-momme silk to a relatively impervious parachute
pack container cloth with reasonably good results, see Figure A-2.

The canopy pressure coefficient, C_p, is defined as the ratio
of the pressure differential across the cloth to the dynamic
pressure of the free stream.

$$C_p = \frac{\Delta P}{q} = \frac{P(\text{internal}) - P(\text{external})}{1/2\rho V^2} \qquad \text{A-1}$$

where V is based on equation (7)

The permeability expression, $P = k(\Delta P)^n$ becomes

$$P = k(C_p \frac{\rho V^2}{2})^n \qquad \text{A-2}$$

Although some progress has been made by Melzig on the measurement
of the variation of the pressure coefficient on an actual inflating
canopy, this dimension and its variation with time are still dark
areas at the time of this writing. At the present time, a constant
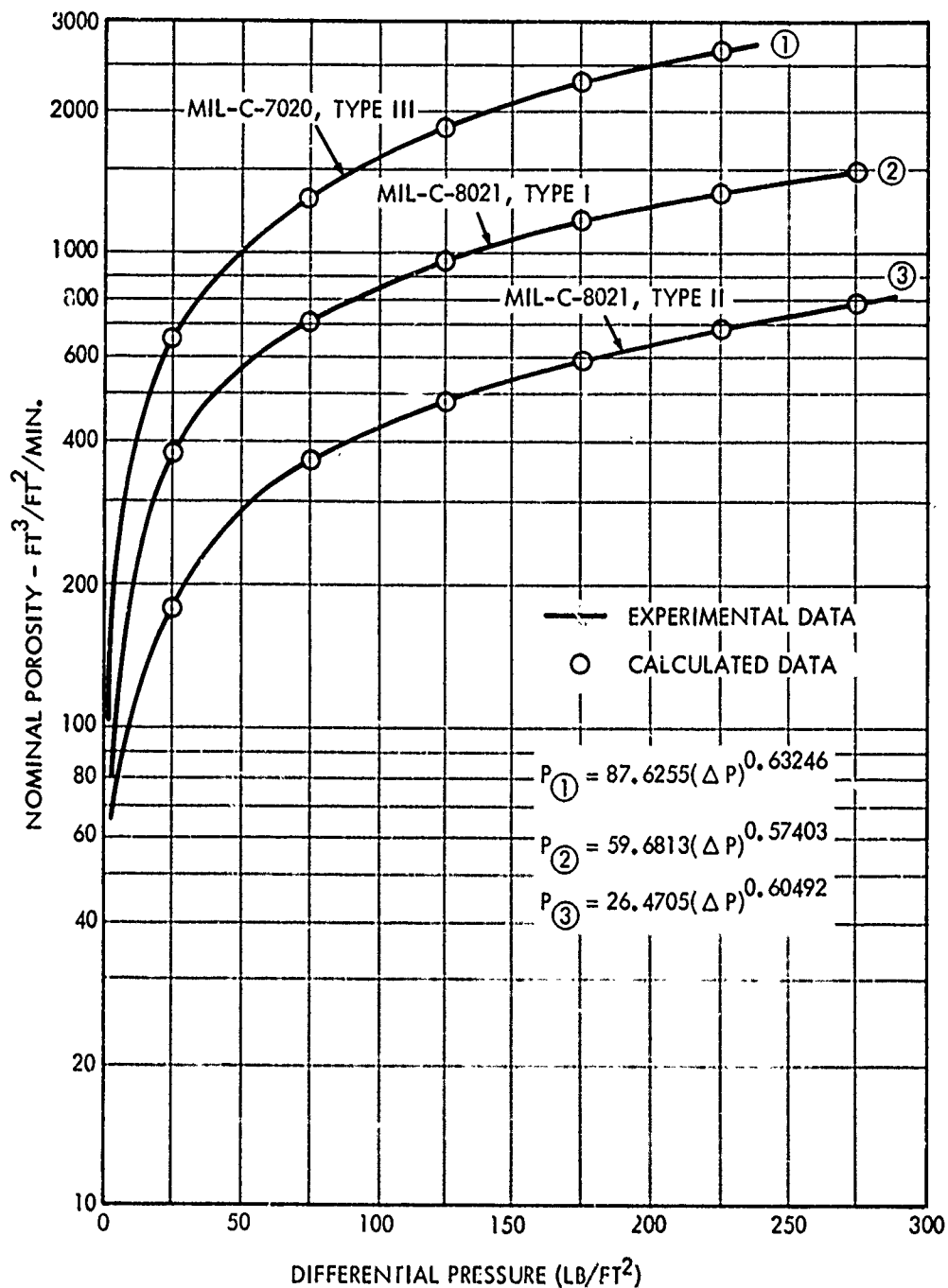
FIG. A-1 NOMINAL POROSITY OF PARACHUTE MATERIAL
VS DIFFERENTIAL PRESSURE

REPRODUCED FROM REFERENCE (4)

3 MOMME SILK CLOTH

$P = k(\Delta P)^n$
$P = 445.521(\Delta P)^{0.612622}$

$\Delta P \quad LB/FT^2$

CONTAINER CLOTH
MIL-C-7219, TYPE II

—— MEASURED DATA
○ CALCULATED DATA

$P = k(\Delta P)^n$
$P = 2.49195(\Delta P)^{0.771591}$

$\Delta P \quad LB/FT^2$

FIG. A-2 COMPARISON OF MEASURED AND CALCULATED PERMEABILITY FOR
RELATIVELY PERMEABLE AND IMPERMEABLE CLOTHS

A-3

average value of pressure coefficient is used in these calculations. Figure A-3 presents the effect of pressure coefficient and altitude on the unfolding time for constant deployment conditions.

It is well known that the inflation time of solid cloth parachutes decreases as the operational altitude increases. This effect can be explained by considering the ratio of the mass outflow through a unit cloth area to the mass inflow through a unit mouth area.

$$M' = \text{mass flow ratio} = \frac{\text{mass outflow}}{\text{mass inflow}}$$

where

$$\text{mass outflow} = P\rho \frac{\text{slugs}}{ft^2\text{-sec}} \ (\text{per } ft^2 \text{ cloth area})$$

and

$$\text{mass inflow} = V\rho \frac{\text{slugs}}{ft^2\text{-sec}} \ (\text{per } ft^2 \text{ inflow area})$$

Therefore, the mass flow ratio becomes

$$M' = \frac{P\rho}{V\rho} = \frac{P}{V}$$

$$M' = k\left(\frac{C_P\rho}{2}\right)^n V^{2n-1} \qquad\qquad A\text{-}3$$

Effective porosity (C) is defined as the ratio of the velocity through the cloth (u) to a fictitious theoretical velocity (v) which will produce the particular $\Delta P = 1/2\rho v^2$.

$$\text{effective porosity, } C = \frac{u}{v} \qquad\qquad A\text{-}4$$

Comparison of the mass flow ratio and previously published effective porosity data is shown in Figure A-4. The effects of altitude and velocity on the mass flow ratio are presented in Figures A-5, A-6, and A-7 for constant velocity, constant dynamic pressure, and constant altitude. The decrease of cloth permeability with altitude is evident.

The permeability constants "k" and "n" can be determined from the permeability-pressure differential data as obtained from an instrument such as a Frazier Permeameter. Two data points, A and B, are selected in such a manner that point "A" is in a low-pressure

AVERAGE CANOPY PRESSURE COEFFICIENT
DURING INFLATION INCLUDING THE VENT
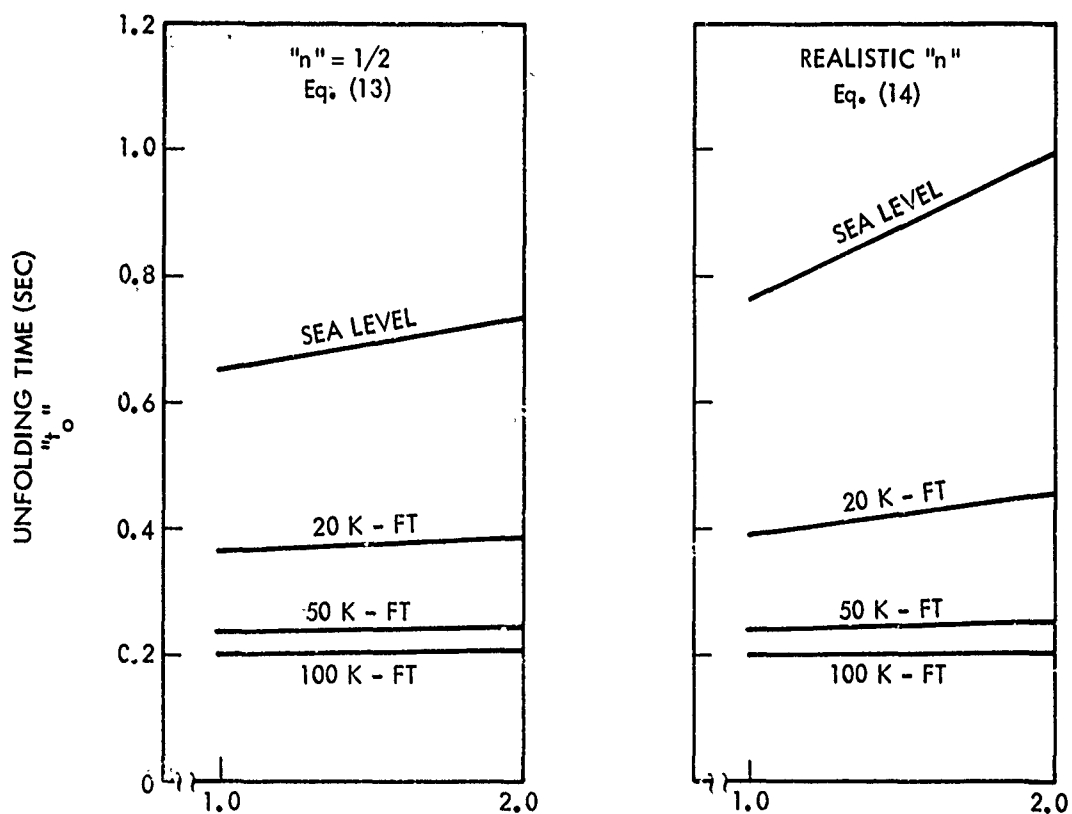
FIG. A-3 EFFECT OF PRESSURE COEFFICIENT AND ALTITUDE ON THE
UNFOLDING TIME
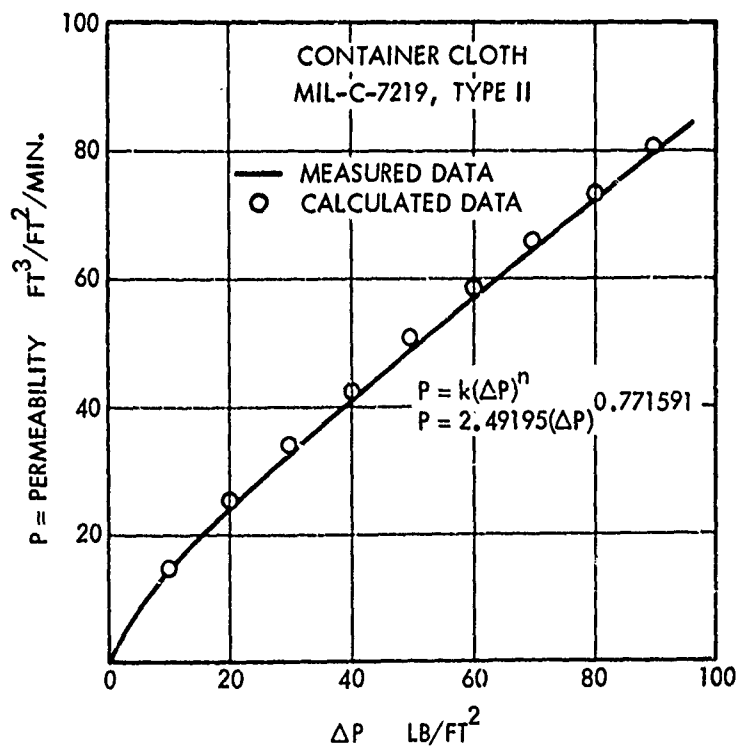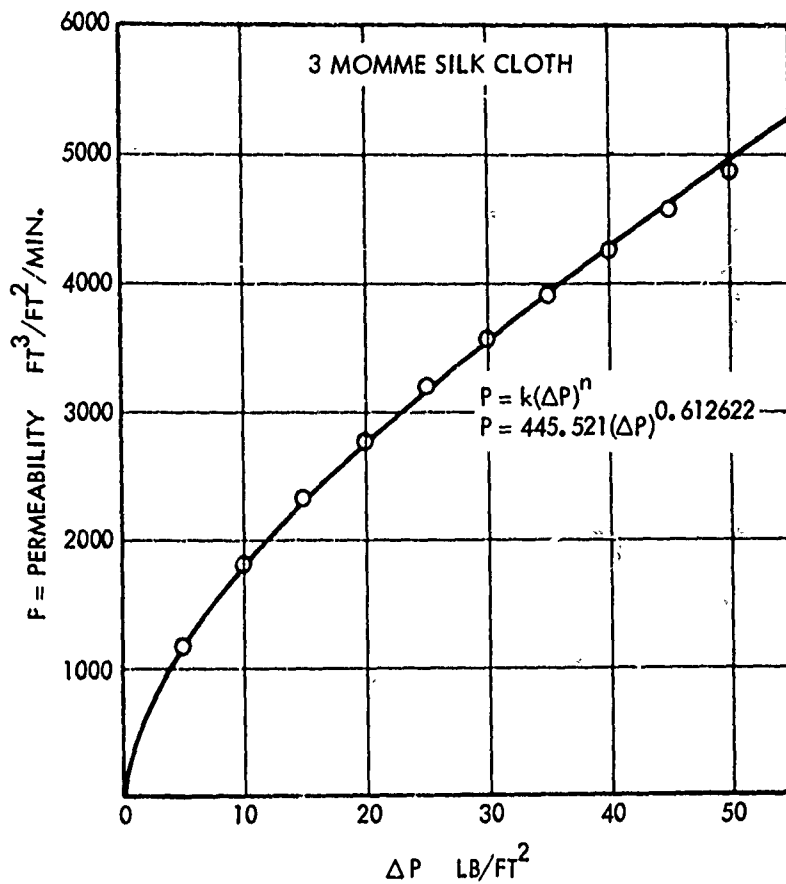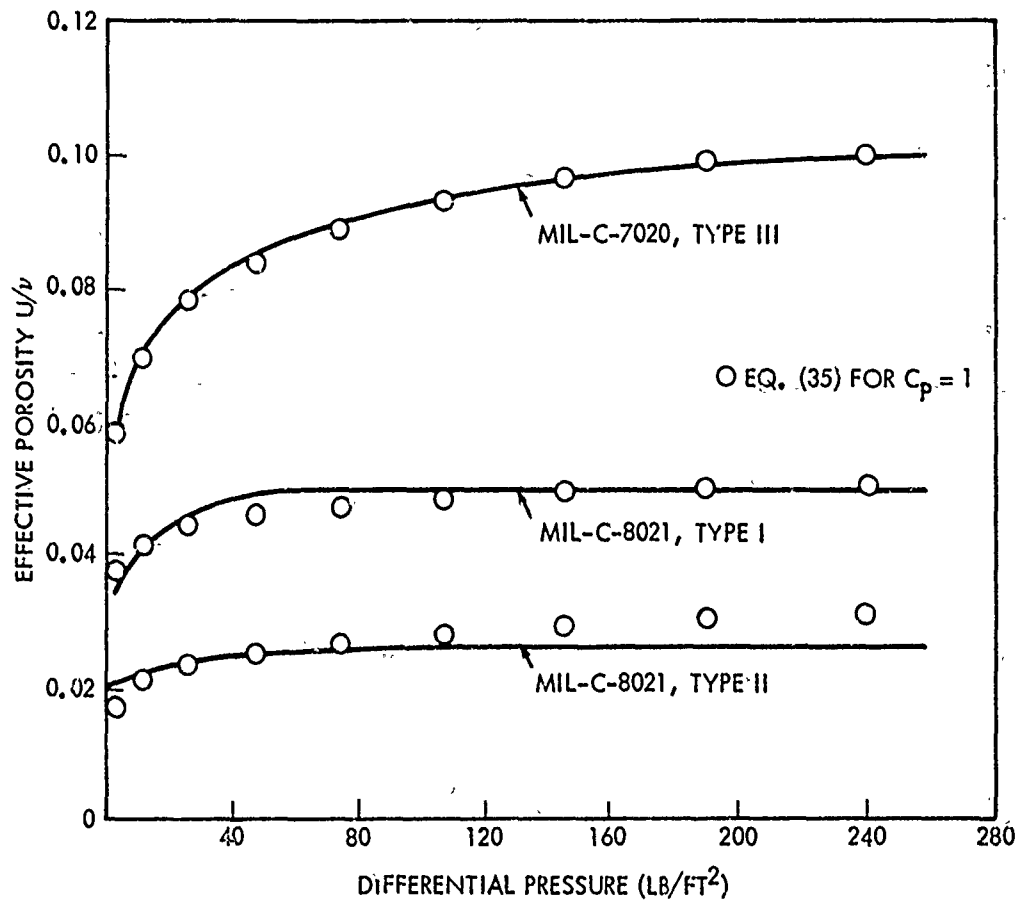
FIG. A-4 THE EFFECTIVE POROSITY OF PARACHUTE MATERIALS VS DIFFERENTIAL
PRESSURE

REPRODUCED FROM REFERENCE (4)

CLOTH, MIL-C-7020, TYPE III

$k = 1.46042;\ n = 0.63246;\ C_p = 1.15$

$M' = \text{MASS FLOW RATIO} = \dfrac{\text{MASS OUTFLOW}}{\text{MASS INFLOW}}$
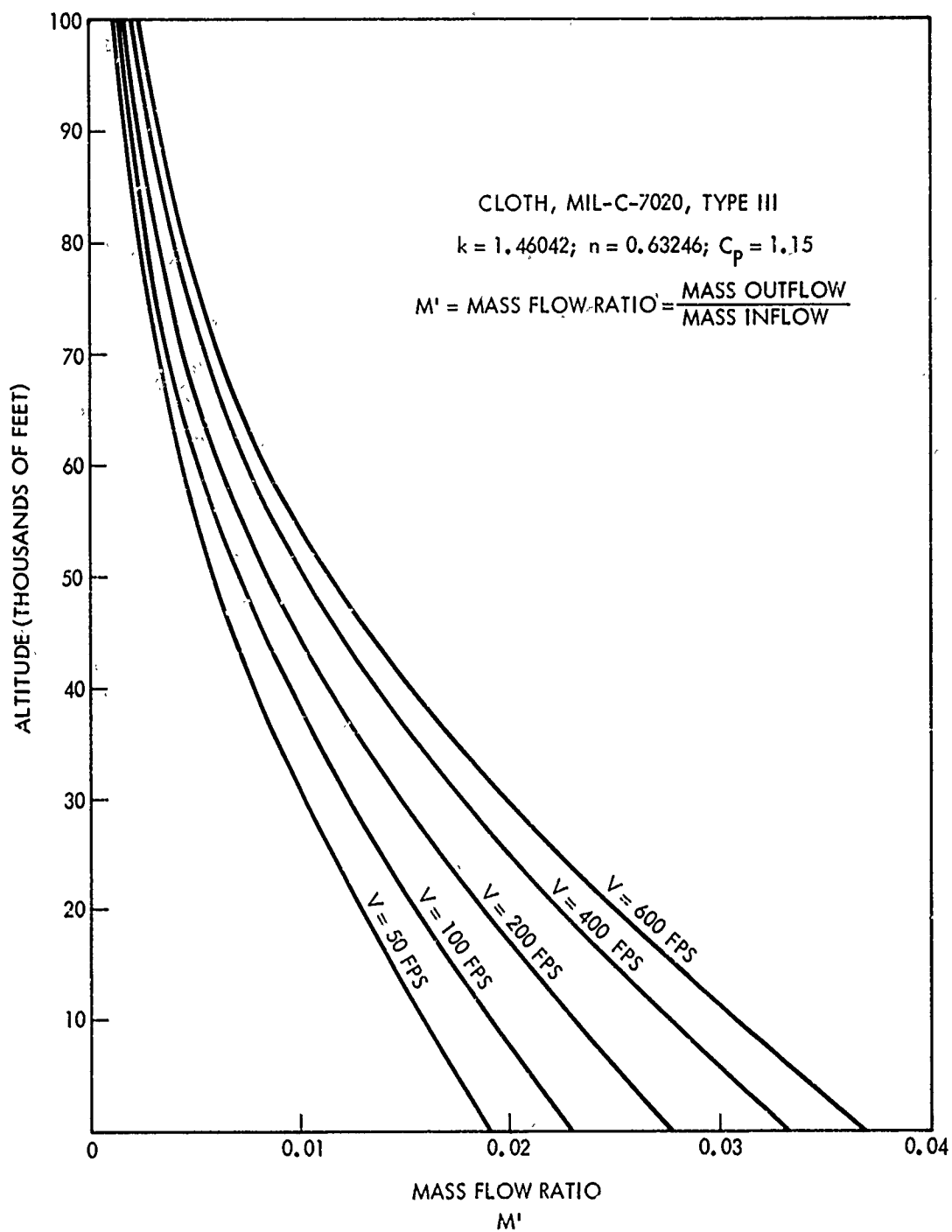
MASS FLOW RATIO
M'

FIG. A-5 EFFECT OF ALTITUDE ON MASS FLOW RATIO AT
CONSTANT VELOCITY

A-7

CLOTH, MIL-C-7020, TYPE III

$k = 1.46042; n = 0.63246; C_p = 1.15$

$M' = \text{MASS FLOW RATIO} = \dfrac{\text{MASS OUTFLOW}}{\text{MASS INFLOW}}$
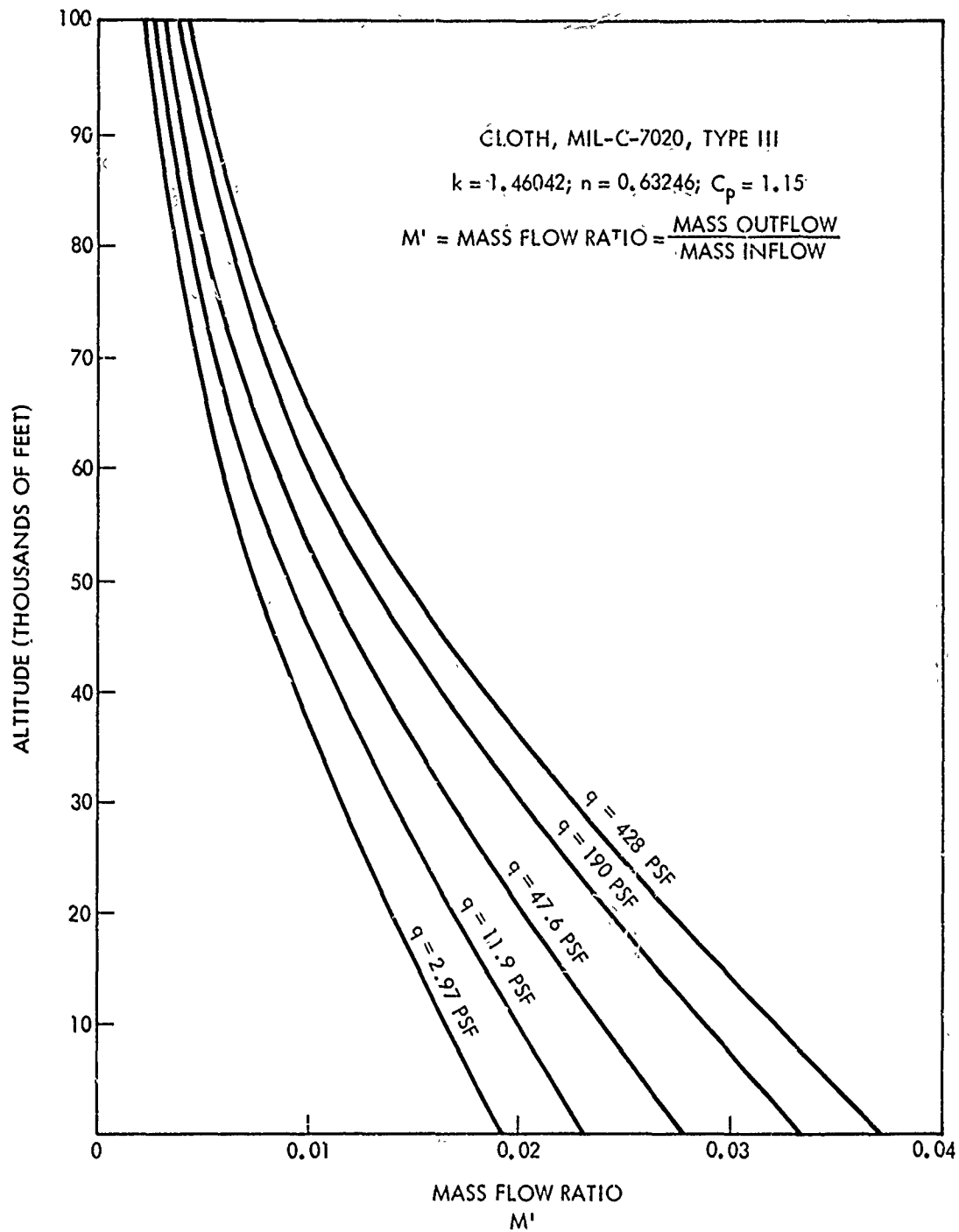
FIG. A-6 EFFECT OF ALTITUDE ON MASS FLOW RATIO AT
CONSTANT DYNAMIC PRESSURE
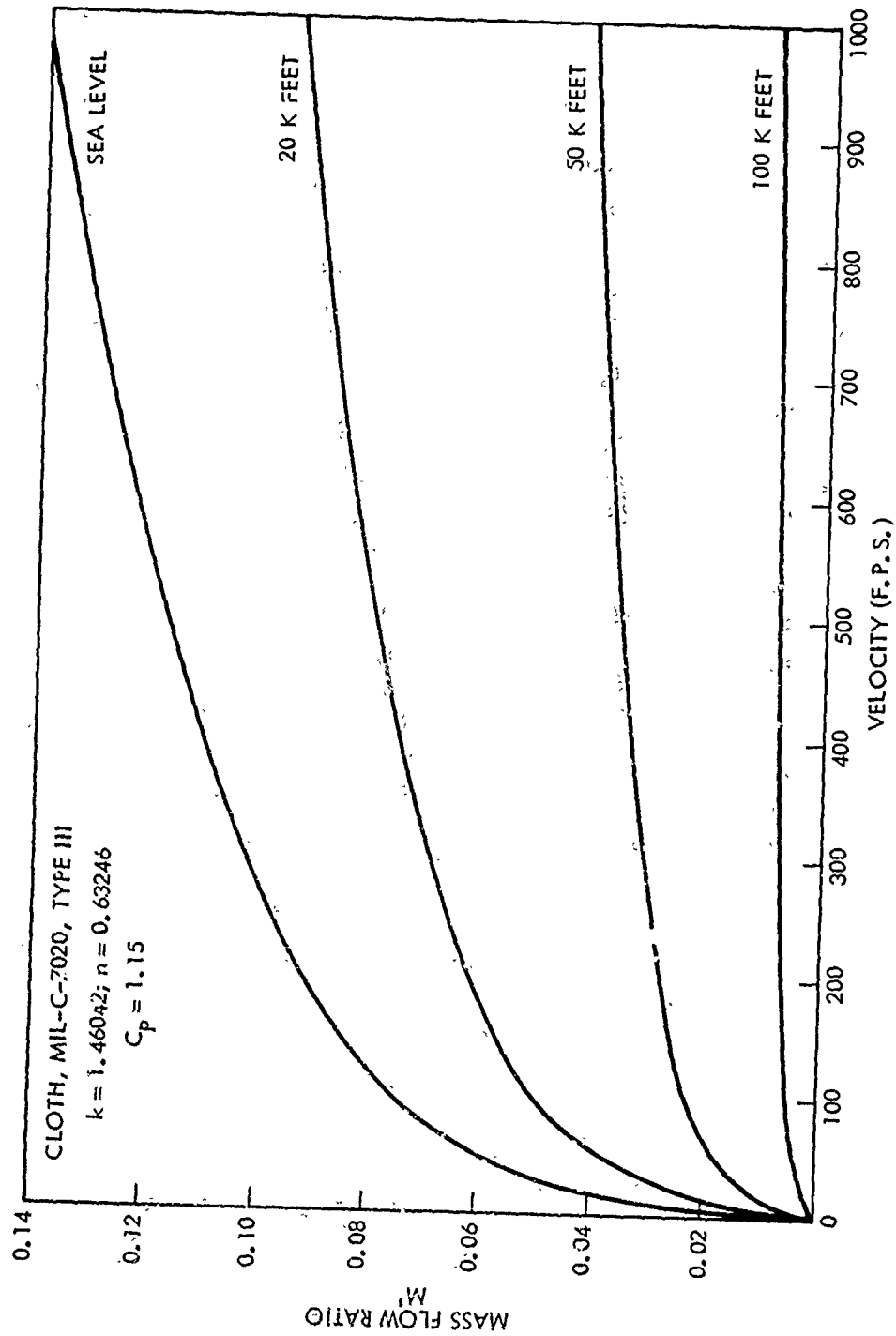
FIG. A-7 EFFECT OF VELOCITY ON MASS FLOW RATIO AT CONSTANT DENSITY

CLOTH, MIL-C-7020, TYPE III

$k = 1.46042; n = 0.63246$

$C_p = 1.15$

zone below the knee of the curve, and point "B" is located in the upper end of the high-pressure zone, as shown in Figure A-8.

$$ P \frac{FT^3}{FT^2 - SEC} $$

POINT "B"

POINT "A"

$$ \Delta P \frac{LB}{FT^2} $$
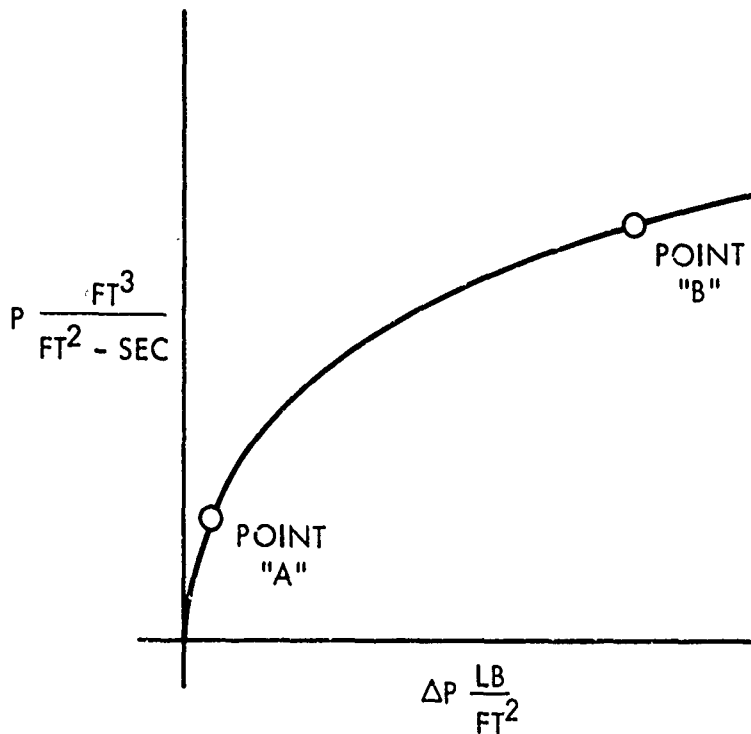
FIG. A-8 LOCATION OF DATA POINTS FOR DETERMINATION OF "k" AND "n"

The two standard measurements of 1/2 inch of water and 20 inches of water appear to be good data points if both are available on the same sample. Substituting the data from points "A" and "B" into $P = k(\Delta P)^n$:

$$ \frac{P_B}{P_A} \qquad \left(\frac{\Delta P_B}{\Delta P_A}\right)^n $$

$$ n \qquad \frac{\ln\left(\dfrac{P_B}{P_A}\right)}{\ln\left(\dfrac{\Delta P_B}{\Delta P_A}\right)} \qquad\qquad A-8 $$

$$k = \frac{P_A}{(\Delta P_A)^n} = \frac{P_B}{(\Delta P_B)^n} \qquad \text{A-6}$$

Theoretically, the inflation characteristics of parachutes can be controlled by designing canopy cloths using predetermined values of the permeability constants "k" and "n." Figure A-9 illustrates the effects of the permeability constants on a given parachute system at various altitudes from sea level through 100,000 feet for a constant deployment velocity. The permeability of the various cloth elements of parachute canopies vary widely. This variation is a source of divergence between calculated and measured inflation time.

FIG.A-9 EFFECT OF CANOPY CLOTH CONSTANTS "k" AND "n"
ON THE UNFOLDING TIME OF A 35-FOOT DIAMETER
10% EXTENDED SKIRT PARACHUTE
V_s = 200 FEET PER SECOND
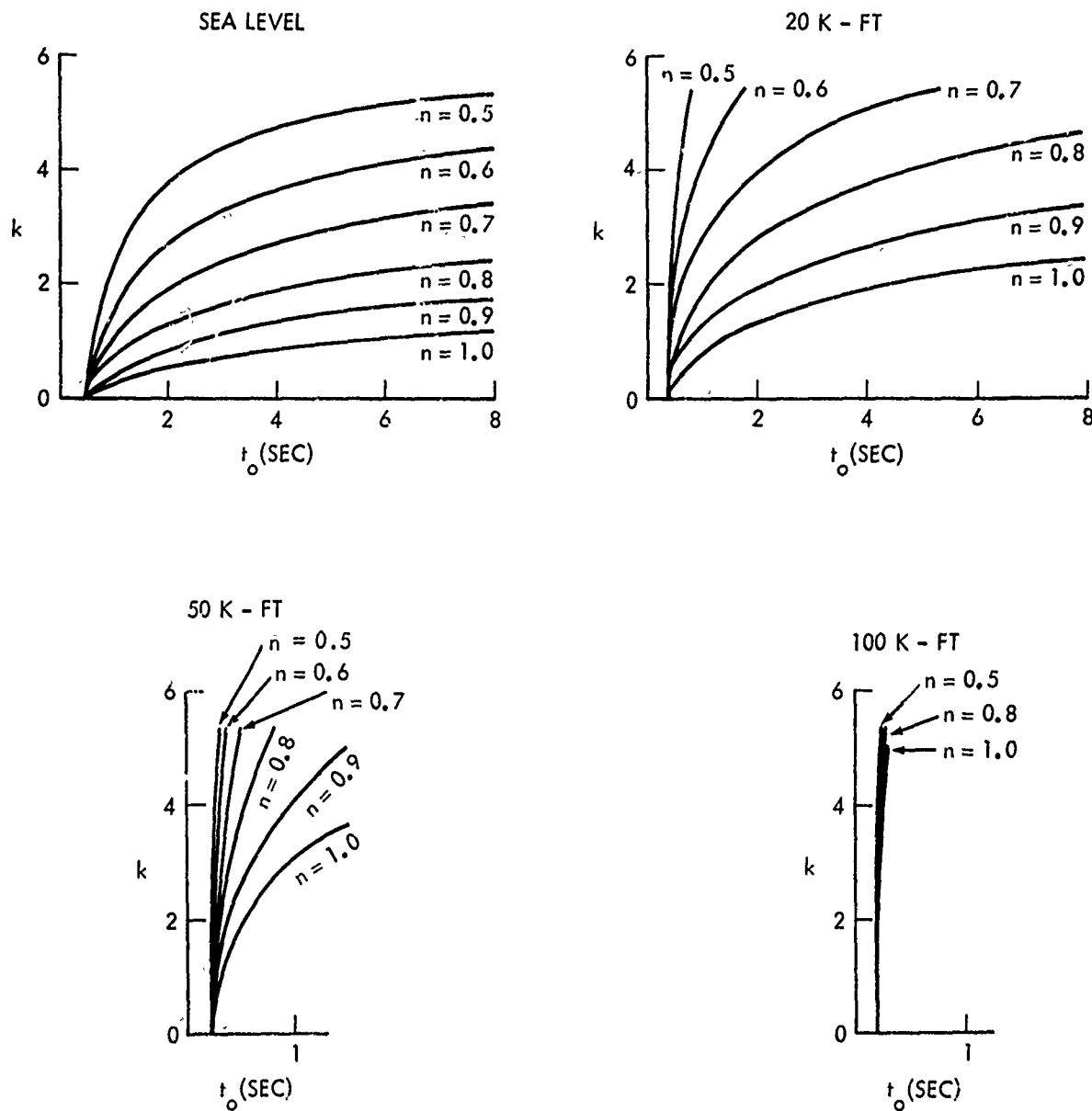
CLOTH	k	n
MIL-C-7020, TYPE III	1.46042	0.63246
MIL-C-8021, TYPE I	0.99469	0.57403
MIL-C-8021, TYPE II	0.44117	0.60492

APPENDIX B

DETERMINATION OF THE PARACHUTE INCLUDED
VOLUME AND ASSOCIATED AIR MASS

Before the reference time, t_o, and inflation time, t_f, can be calculated, the volume of atmosphere, V_o, which is to be collected during the inflation process must be accurately known. This requirement dictates that a realistic inflated canopy shape and associated volume of atmosphere be determined. Figure B-1 was reproduced from reference (5). The technique of using lampblack coated plates to determine the airflow patterns around metal models of inflated canopy shapes was used by the investigator of reference (5) to study the stability characteristics of contemporary parachutes, i.e., 1943. A by-product of this study is that it is clearly shown that the volume of air within the canopy bulges out of the canopy mouth (indicated by arrows) and extends ahead of the canopy hem. This volume must be collected during the inflation process. Another neglected, but significant, source of canopy volume exists in the billowed portion of the gore panels.

The steady-state canopy shape has been observed in wind-tunnel and field tests to be elliptical in profile. Studies of the inflated shape and included volume of several parachute types (flat circular, 10 percent extended skirt, elliptical, hemispherical, ring slot, ribbon, and cross) are documented in references (6) and (7). These studies demonstrated that the steady-state profile shape of inflated canopies of the various types can be approximated to be two ellipses of common major diameter, $2\bar{a}$, and dissimilar minor diameters, b and b', as shown in Figure B-2. It was also shown that the volume of the ellipsoid of revolution formed by revolving the profile shape about the canopy axis was a good approximation of the volume of atmosphere to be collected during canopy inflation and included the air volume extended ahead of the parachute skirt hem together with the billowed gore volume.

$$V_o = \frac{2}{3} \pi \bar{a}^3 \left[\frac{b}{\bar{a}} + \frac{b'}{\bar{a}} \right] \qquad \text{B-1}$$

Tables B-I and B-II are summaries of test results reproduced from references (6) and (7), respectively, for the convenience of the reader.
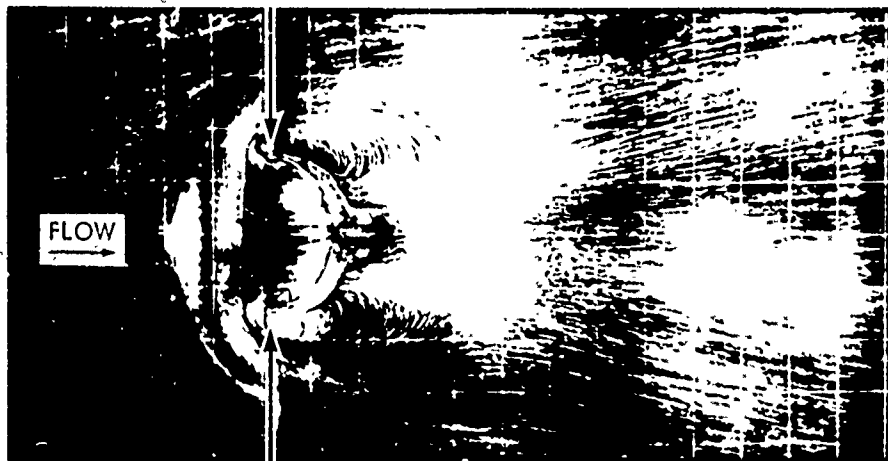
HEMISPHERE
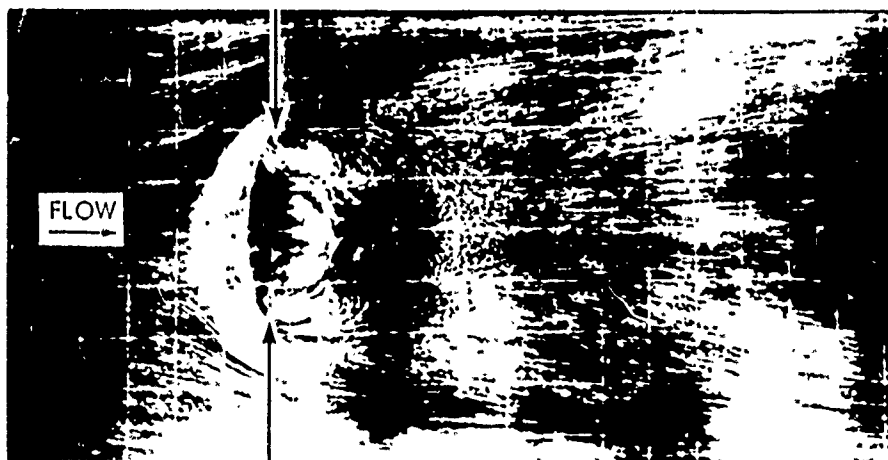
VENT PARACHUTE

REPRODUCED FROM REFERENCE (5)

FIG.B-1 AIRFLOW PATTERNS SHOWING AIR VOLUME AHEAD OF CANOPY HEM

FIG. B-2 PARACHUTE CROSS SECTION NOMENCLATURE

REPRODUCED FROM REFERENCE (6)

TABLE B-1

SUMMARY OF PARACHUTE SHAPE TEST RESULTS FOR
12-GORE AND 16-GORE CONFIGURATIONS

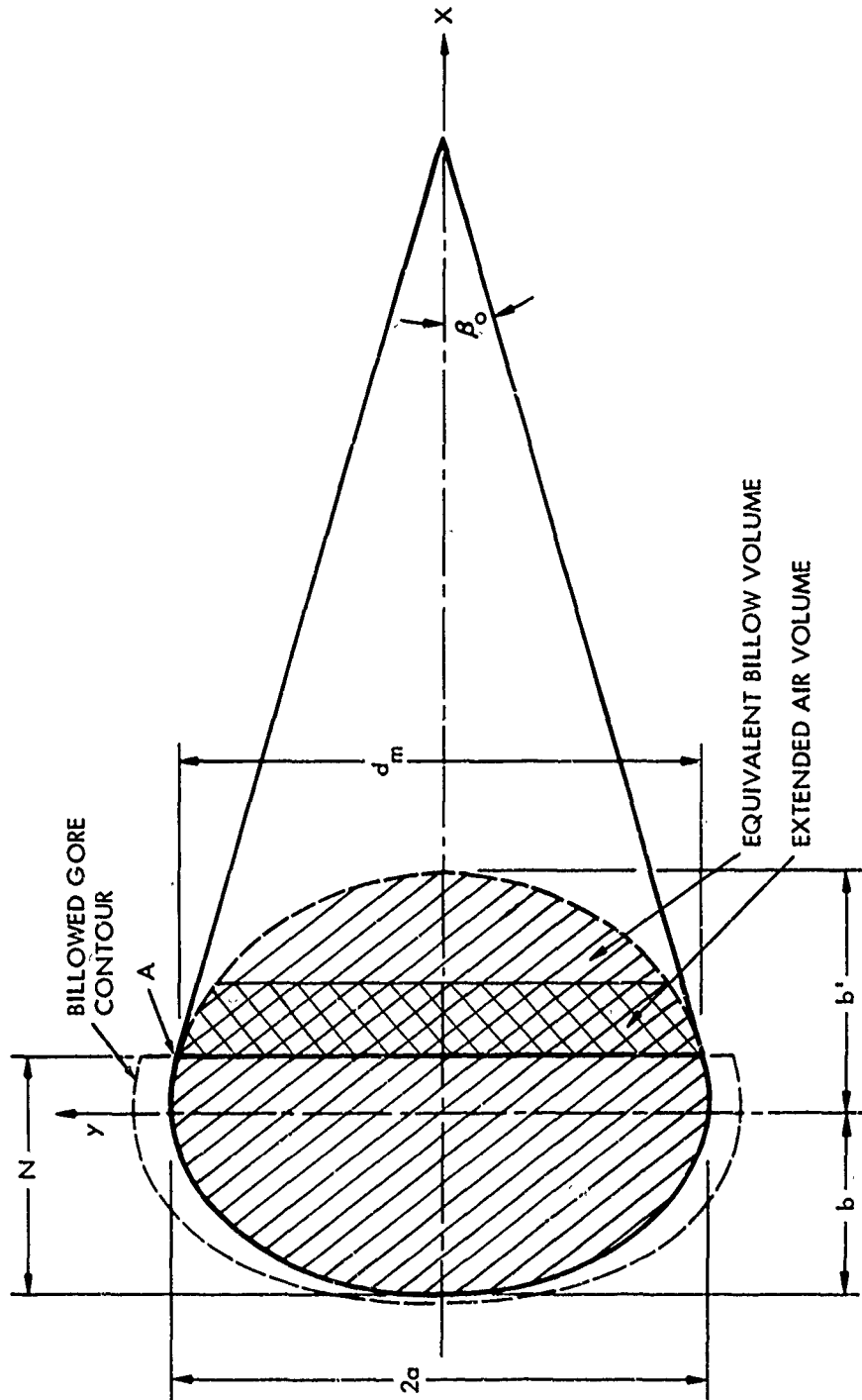| Parachute Type	No. of Gores	Suspension Line Length inches	Velocity mph	Velocity fps	$2\bar{a}/\bar{D}_o$	$2\bar{a}/\bar{D}_F$	$2\bar{a}/\bar{D}_R$	$2\bar{a}/\bar{L}$	$Z/\bar{a}$	$b/\bar{a}$	$b'/\bar{a}$	$(b+b')/\bar{a}$	V_H	V_c	V_o	V_o/V_H
Flat Circular	12	34	50	73	.645	.650			.856	.6115	.8817	1.4932	4476	4481	6980	1.56
	16	34	50	73	.663	.669			.820	.5558	.9039	1.4597	4450	4100	7325	1.65
10% Extended Skirt	12	34	100	147	.663	.652			.881	.6424	.8360	1.5284	3928	4400	6783	1.73
	16	34	17	25	.654	.640			.785	.5580	.8502	1.4082	4051	3920	6197	1.53
Elliptical	12	34	75	110			.916		.812	.5826	.9657	1.5283		3322	5405	
	16	34	17	25			.875		.800	.6169	.8163	1.4332		2726	4405	
Hemispherical	12	34	125	183			.996		1.254	1.0005	.9080	1.9085		6224	8666	
	16	34	75	110			.894		1.185	.9129	.9380	1.8509		5921	8370	
Ringslot 16% Geometric Porosity	12	34	25	37	.607	.654			.853	.6566	.8735	1.530	3800	3650	5903	1.55
	12	34	100	147	.616	.663			.922	.6566	.8735	1.530	3800	4198	6166	1.62
	12	34	200	293	.637	.686			.918	.6566	.8735	1.530	3800	4624	6826	1.90
	16	34	25	37	.611	.658			.827	.6004	.8890	1.4894	3800	3673	5685	1.50
	16	34	100	147	.617	.664			.864	.6004	.8890	1.4894	3800	3985	6030	1.59
	16	34	200	293	.645	.695			.844	.6004	.8890	1.4894	3800	4430	6897	1.82
Ribbon 24% Geometric Porosity	12	34	25	37	.586	.632			.859	.6558	.8768	1.5326	3800	3323	5335	1.40
	12	34	100	147	.615	.663			.837	.6558	.8768	1.5326	3800	3714	6163	1.62
	12	34	200	293	.632	.681			.877	.6558	.8768	1.5326	3800	4280	6683	1.76
	16	34	25	37	.603	.650			.797	.5570	.8578	1.4148	3800	3438	5358	1.41
	16	34	100	147	.626	.674			.791	.5570	.8578	1.4148	3800	3804	5983	1.57
	16	34	200	293	.648	.698			.781	.5570	.8578	1.4148	3800	4164	6656	1.75
Cross Chute w/L = .264		34	25	37	.710			.563	1.242	.8867	1.2776	2.1643	1928	3768	5798	3.01
		34	100	147	.707			.540	1.270	.8867	1.2776	2.1643	1928	3810	5712	2.96
		34	200	293	.716			.547	1.285	.8867	1.2776	2.1643	1928	4212	5925	3.07
		47	25	37	.759			.580	1.113	.8494	1.2512	2.1006	1928	4052	6868	3.56
		47	100	147	.729			.557	1.205	.8494	1.2512	2.1006	1928	3973	5938	3.09
		47	200	293	.775			.592	1.110	.8494	1.2512	2.1006	1928	4292	7303	3.79

TABLE B-2.

SUMMARY OF PARACHUTE SHAPE TEST RESULTS FOR
24-GORE AND 30-GORE CONFIGURATIONS

Parachute Type	No. of Gores	Suspension Line Length inches	Velocity mph	fps	Scale Factor, K $\frac{2\bar{a}}{D_o}$	$\frac{2\bar{a}}{D_F}$	$\frac{N}{\bar{a}}$	Axes Ratio $\frac{b}{\bar{a}}$	$\frac{b'}{\bar{a}}$	$\frac{b+b'}{\bar{a}}$	Volume in³ V_H	V_c	V_o	$\frac{V_o}{V_H}$
Flat Circular*	24	34	50	73	.677	.679	.795	.5758	.8126	1.3884	4362	4685	7273	1.67
	30	34	17	25	.668	.669	.827	.6214	.7806	1.4020	4342	4626	7027	1.62
10% Extended* Skirt	24	34	100	147	.665	.648	.834	.5949	.8771	1.4720	4138	4446	6930	1.67
	30	34	17	25	.630	.633	.625	.6255	.7962	1.4127	4172	4076	6265	1.50
Ring Slot 16%	24	34	25	37	.663	.665	.824	.5800	.9053	1.4853	3591	3878	6031	1.68
Geometrically	24	34	100	147	.680	.682	.819	.5800	.9053	1.4853	3591	4079	6510	1.81
Porous	24	34	200	293	.694	.696	.809	.5800	.9053	1.4853	3591	4270	6924	1.93
	30	34	25	37	.677	.678	.788	.5800	.9053	1.4853	3582	3826	6404	1.79
	30	34	100	147	.684	.685	.802	.5800	.9053	1.4853	3582	4023	6508	1.84
	30	34	200	293	.698	.699	.800	.5800	.9053	1.4853	3582	4260	7012	1.96
Ribbon 24%	24	34	25	37	.671	.673	.770	.5980	.8187	1.4167	3591	3591	5968	1.66
Geometrically	24	34	100	147	.676	.678	.813	.5980	.8187	1.4167	3591	3927	6097	1.70
Porous	24	34	200	293	.687	.689	.804	.5980	.8187	1.4167	3591	4061	6389	1.78
	30	34	25	37	.655	.657	.782	.6021	.8463	1.4484	3582	3396	5666	1.58
	30	34	100	147	.669	.670	.784	.6021	.8463	1.4484	3582	3622	6022	1.68
	30	34	200	293	.677	.679	.823	.6021	.8463	1.4484	3582	4002	6256	1.75

*Since this parachute was "breathing" during the test, several photographs were taken at each speed. The data were reduced from the photograph which most reasonably appeared to represent the equilibrium state.